

Supporting Information For

Cross-linked AIE supramolecular polymer gels with multiple stimuli-responsive behaviours constructed by hierarchical self-assembly

Chang-Wei Zhang,^a Bo Ou,^a Shu-Ting Jiang,^a Guang-Qiang Yin,^a Li-Jun Chen,^a Lin Xu,^{*a} Xiaopeng Li,^b and Hai-Bo Yang^{*a}

^a*Shanghai Key Laboratory of Green Chemistry and Chemical Processes, School of Chemistry and Molecular Engineering, East China Normal University, Shanghai 200062, P. R. China.*

E-mail: lxu@chem.ecnu.edu.cn; hbyang@chem.ecnu.edu.cn

^b*Department of Chemistry, University of South Florida, Tampa, Florida 33620, United States*

Table of Contents:

1. General Information.....	2
2. Experimental details for synthesis and characterization of new compounds	3
Synthesis of compound 2	3
Synthesis of compound H1	3
Synthesis of rhombic metallacycle H2	4
Synthesis of hexagonal metallacycle H3	5
3. X-ray Crystal Data of 2	6
4. The simulated molecular model of H1 , H2 and H3	7
5. 2-D ¹ H- ¹ H NOESY NMR spectra of H2 and H3 in acetone- <i>d</i> ₆	9
6. Photophysical investigation of H2 and H3	10
7. Host-guest complexation studies in dilute solution.	10
7. Cross-linked supramolecular polymers constructed through host-guest interactions.....	11
8. Stimuli-responsive supramolecular polymer gels.....	14
9. Multiple nuclear NMR (¹ H, ³¹ P, ¹⁹ F, and ¹³ C NMR) spectra of new compounds	19
11. MS Spectra of New Compounds.....	24

1. General Information.

The compounds **1^{S1}** and **3^{S2}**, organoplatinum 60° acceptor **A1^{S1}** and organoplatinum 120° acceptor **A2^{S4}**, were prepared as the reported procedures in literatures. Solvents were either employed as purchased or dried according to procedures described in the literature.

¹H NMR, ¹³C NMR, ³¹P NMR, and ¹⁹F NMR spectra were recorded on Bruker 400 MHz Spectrometer (¹H: 400 MHz; ¹³C: 100 MHz; ³¹P: 161.9 MHz) and Bruker 500 MHz Spectrometer (¹H: 500 MHz) at 298 K. The ¹H and ¹³C NMR chemical shifts are reported relative to residual solvent signals, and ³¹P NMR resonances are referenced to a internal standard sample of 85% H₃PO₄ (δ 0.0). Coupling constants (*J*) are denoted in Hz and chemical shifts (δ) in ppm. Multiplicities are denoted as follows: s = singlet, d = doublet, m = multiplet, br = broad. IR spectra were recorded on a Bruker Tensor 27 infrared spectrophotometer.

Dynamic Light Scattering (DLS) Studies. DLS measurements were performed under a Malvern Zetasizer Nano-ZS light scattering apparatus (Malvern Instruments, U.K.) with a He-Ne laser (633 nm, 4 mW).

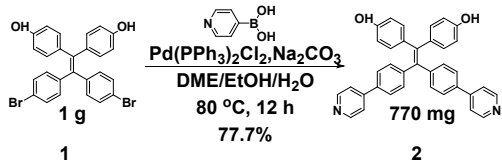
Transmission Electron Microscopy (TEM) Experiments. TEM images were recorded on a Tecnai G2 F30 (FEI Ltd.). The sample for TEM measurements was prepared by dropping the solution onto a carbon-coated copper grid.

Scanning Electron Microscopy (SEM) Experiments. The SEM samples were prepared on clean Si substrates. To minimize sample charging, a thin layer of Au was deposited onto the samples before SEM examination. All the SEM images were obtained using an S-4800 (Hitachi Ltd.) with an accelerating voltage of 3.0-10.0 kV.

Rheological Experiments. Rheological measurements were performed under a MARS III (HAAKE MARS III) device at 293K.

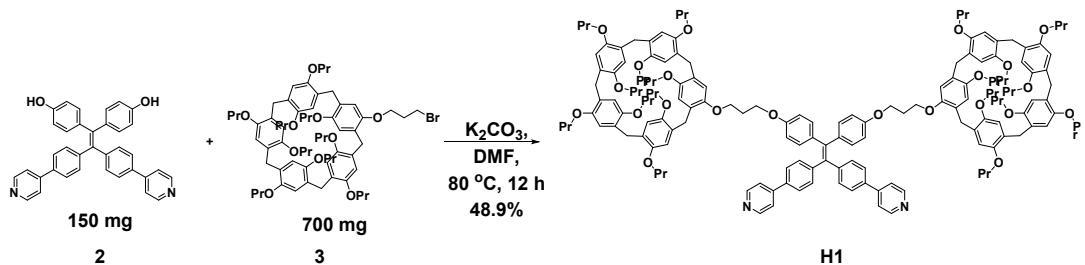
2. Experimental details for synthesis and characterization of new compounds

Scheme S1 Synthesis route of compound **2**.



Synthesis of compound 2. A 200 mL Schlenk flask was charged with compound **1** (1 g, 1.91 mmol), degassed, and back-filled three times with N₂. Anhydrous DME (1, 2-Dimethoxyethane) (15 mL) was introduced into the reaction flask by syringe. Then Pd(PPh₃)₂Cl₂ (667 mg, 0.95 mmol) was added into the flask under nitrogen atmosphere. Then an ethanol solution of Pyridin-4-ylboronic acid (1.41 g, 11.46 mmol in 20 mL ethanol) and aqueous Na₂CO₃ (1.7 g, 16 mmol in 10 mL water) was introduced into the reaction flask by syringe. The solution was heated under an inert atmosphere at 80 °C for 16 h, cooled to room temperature and added to EtOAc (100 mL). The solution was washed with H₂O (2 × 100 mL) and brine (100 mL), dried by Na₂SO₄. Then the solvent was removed by evaporation on a rotary evaporator. The residue was purified by column chromatography on silica gel to give compound **2** as a gold yellow solid. Yield: 0.77 g, 77.7 %. R_f = 0.44 (ethyl acetate). Mp: >300 °C. ¹H NMR (DMSO, 400 MHz): δ 9.39 (s, 2H), 8.58 (d, J = 5.9 Hz, 4H), 7.66 (dd, J = 9.9, 7.2 Hz, 8H), 7.10 (d, J = 8.3 Hz, 4H), 6.81 (d, J = 8.5 Hz, 4H), 6.53 (d, J = 8.5 Hz, 4H); ¹³C NMR (DMSO, 125 MHz): δ 156.2, 150.2, 146.2, 145.2, 142.2, 136.2, 134.3, 133.8, 132.2, 131.7, 126.2, 120.8, 114.7. IR (neat): 1559, 1506, 1439, 1266, 1166, 999, 813 cm⁻¹. MS (EI): 518 (M⁺, 100), 519 (31), 44 (25), 43 (11), 77 (10), 91 (10), 55 (10), 93 (9); HRMS (EI): Exact mass calcd for C₃₆H₂₆N₂O₂ [M]⁺: 518.1994, Found: 518.1992.

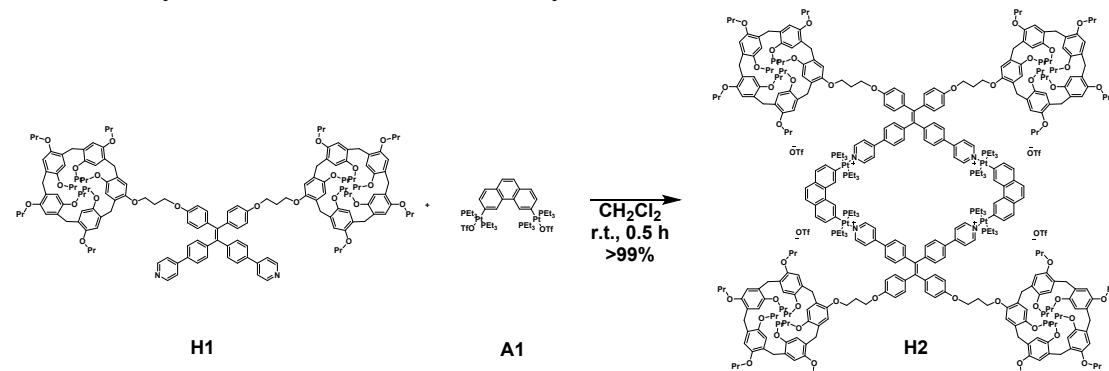
Scheme S2 Synthesis route of compound **H1**.



Synthesis of compound H1. A solution of compound **2** (150 mg, 0.29 mmol) and K₂CO₃ (373 mg, 2.7 mmol) in anhydrous DMF (15 mL) was heated at 80 °C for 5 min, and then monofunctionalized pillar[5]arene **3** (700 mg, 0.63 mmol) was added under nitrogen atmosphere.

The solution was heated at 80 °C for 12 h. After the solid was filtered, the remaining solution was added to EtOAc (50 mL) and washed with H₂O (3×50 mL). The organic layer was dried over anhydrous Na₂SO₄. Then the solvent was removed by evaporation on a rotary evaporator. The residue was purified by column chromatography on silica gel to give compound **H1** as a yellow solid. Yield: 360 mg, 48.5%. *Rf* = 0.44 (petroleum ether/ethyl acetate = 1: 1). Mp: 118 °C. ¹H NMR (CD₂Cl₂, 400 MHz): δ 8.59 (d, *J* = 5.9 Hz, 4H), 7.57 – 7.37 (m, 8H), 7.19 (d, *J* = 8.3 Hz, 4H), 7.00 (d, *J* = 8.6 Hz, 4H), 6.95 – 6.78 (m, 20H), 6.72 (d, *J* = 8.7 Hz, 4H), 4.18 (t, *J* = 6.1 Hz, 4H), 4.06 (s, 4H), 3.76 (m, 56H), 2.35 – 2.23 (m, 4H), 1.97 – 1.71 (m, 36H), 1.08 (m, 54H); ¹³C NMR (CD₂Cl₂, 125 MHz): δ 158.4, 150.6, 150.2, 150.0, 149.6, 147.9, 145.7, 142.3, 137.9, 136.3, 136.0, 133.0, 132.5, 128.7, 128.6, 128.5, 128.4, 126.7, 121.5, 114.4, 114.1, 70.1, 65.4, 65.3, 30.3, 29.6, 29.5, 23.6, 11.0, 10.9. IR (neat): 2961, 2856, 1594, 1500, 1407, 1202, 1064, 989 cm⁻¹. MOLDI-TOF-MS of compound **H1**: m/z calcd for C₁₆₆H₂₀₂N₂O₂₂ ([M+H]⁺): 2576.47, found: 2576.89. Anal. Calcd for C₁₆₆H₂₀₂N₂O₂₂: C, 77.36; H, 7.90; N, 1.09. Found: C, 77.09; H, 7.92; N, 1.15.

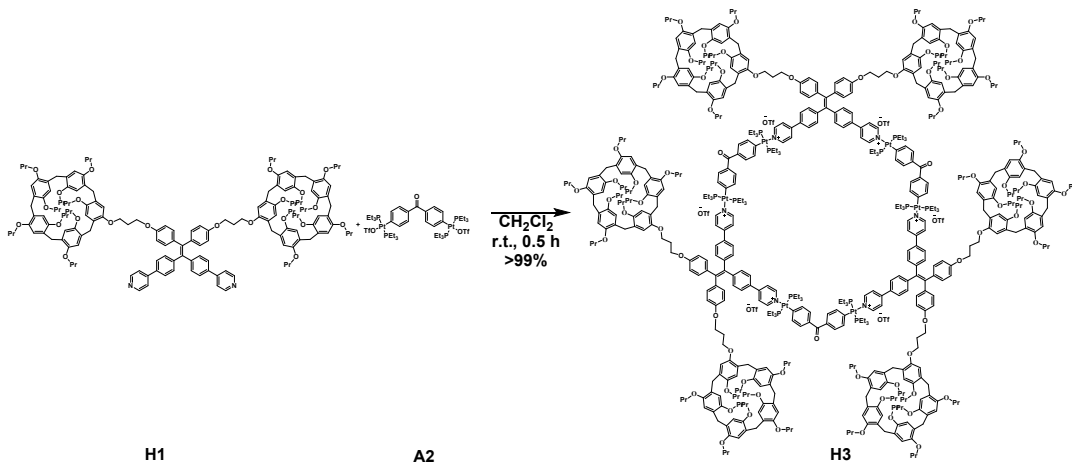
Scheme S3 Synthesis route of rhombic metallacycle **H2**.



Synthesis of rhombic metallacycle **H2.** The dipyridyl donor ligand **H1** (26.85 mg, 10.42 μmol) and the organoplatinum 60° acceptor **A1** (13.93 mg, 10.42 μmol) were weighed accurately into a glass vial. To the vial was added 1 mL of dichloromethane solvent, and the reaction solution was then stirred at room temperature for 0.5 h to yield a homogeneous pale yellow solution. Yellow solid product **H2** was obtained by removing the solvent under vacuum. Yield: 40.78 mg, >99%. Mp: 212 °C. ¹H NMR (CD₂Cl₂, 400 MHz): δ 8.93 (s, 2H), 8.63 (s, 4H), 8.05 (s, 2H), 7.90 (s, 2H), 7.77 – 7.49 (m, 10H), 7.29 (d, *J* = 3.8 Hz, 4H), 7.13 – 6.99 (m, 4H), 6.89 (br, 20H), 6.79 – 6.62 (m, 4H), 4.19 (s, 4H), 4.06 (s, 4H), 4.04 – 3.50 (br, 56H), 2.30 (s, 4H), 1.84 (br, 36H), 1.34 (br, 24H), 1.27 – 0.93 (m, 90H); ³¹P NMR (CD₂Cl₂, 161.9 MHz): δ 13.17 (s, *J*_{Pt-P} = 2698.1 Hz). IR

(neat): 2961, 2923, 2875, 1609, 1499, 1408, 1260, 1202, 1030 cm⁻¹. ESI-TOF-MS of **H2**: calcd for [M – 3OTf]³⁺: 2463.2285, found: 2463.0508; calcd for [M – 5OTf]⁴⁺: 1809.1736, found: 1809.1692.

Scheme S4 Synthesis route of hexagonal metallacycle **H3**



Synthesis of hexagonal metallacycle **H3.** The dipyridyl donor ligand **H1** (19.66 mg, 7.63 μmol) and the organoplatinum 120° acceptor **A2** (10.23 mg, 7.63 μmol) were weighed accurately into a glass vial. To the vial was added 1 mL of dichloromethane solvent, and the reaction solution was then stirred at room temperature for 0.5 h to yield a homogeneous pale yellow solution. Yellow solid product **H3** was obtained by removing the solvent under vacuum. Yield: 29.88 mg, >99%. Mp: 238 °C. ^1H NMR (CD_2Cl_2 , 400 MHz): δ 8.63 (s, 4H), 7.94 (d, $J = 5.4$ Hz, 4H), 7.69 (d, $J = 8.1$ Hz, 4H), 7.61 – 7.44 (m, 8H), 7.28 (d, $J = 8.1$ Hz, 4H), 7.04 (d, $J = 8.3$ Hz, 4H), 6.99 – 6.78 (br, 20H), 6.75 (d, $J = 8.3$ Hz, 4H), 4.20 (s, 4H), 4.06 (s, 4H), 3.79 (br, 56H), 2.31 (s, 4H), 1.85 (br, 36H), 1.36 (br, 24H), 1.25 – 0.92 (br, 91H); ^{31}P NMR (CD_2Cl_2 , 161.9 MHz): δ 13.25 (s, $J_{\text{Pt-P}} = 2663.2$ Hz). IR (neat): 2963, 1741, 1726, 1377, 1259, 1013, 790 cm⁻¹. ESI-TOF-MS of **H3**: calcd for [M – 4OTf]⁵⁺: 2203.9028, found: 2203.8577; calcd for [M – 5OTf]⁶⁺: 1811.0909, found: 1811.0906.

Reference:

- S1. M. Zhang, S. Li, X. Yan, Z. Zhou, M. L. Saha, Y. Wang and P. J. Stang, *Proc. Natl. Acad. Sci. U. S. A.*, 2016, **113**, 11100.
- S2. C.-W. Zhang, B. Ou, G.-Q. Yin, L.-J. Chen, H.-B. Yang, *Acta Polym. Sin.* 2017, (1): 71.
- S3. S. Leininger, M. Schmitz and P. J. Stang, *Org. Lett.*, 1999, **1**, 1921.

3. X-ray Crystal Data of 2

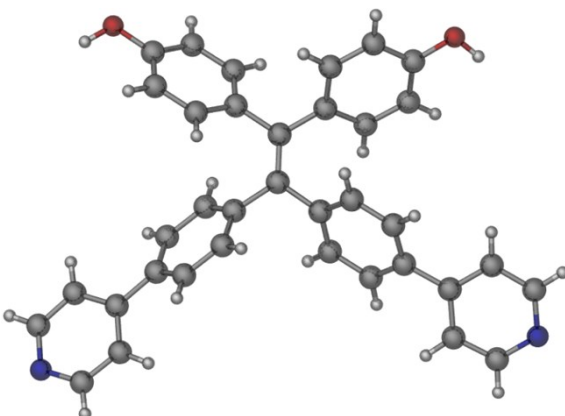
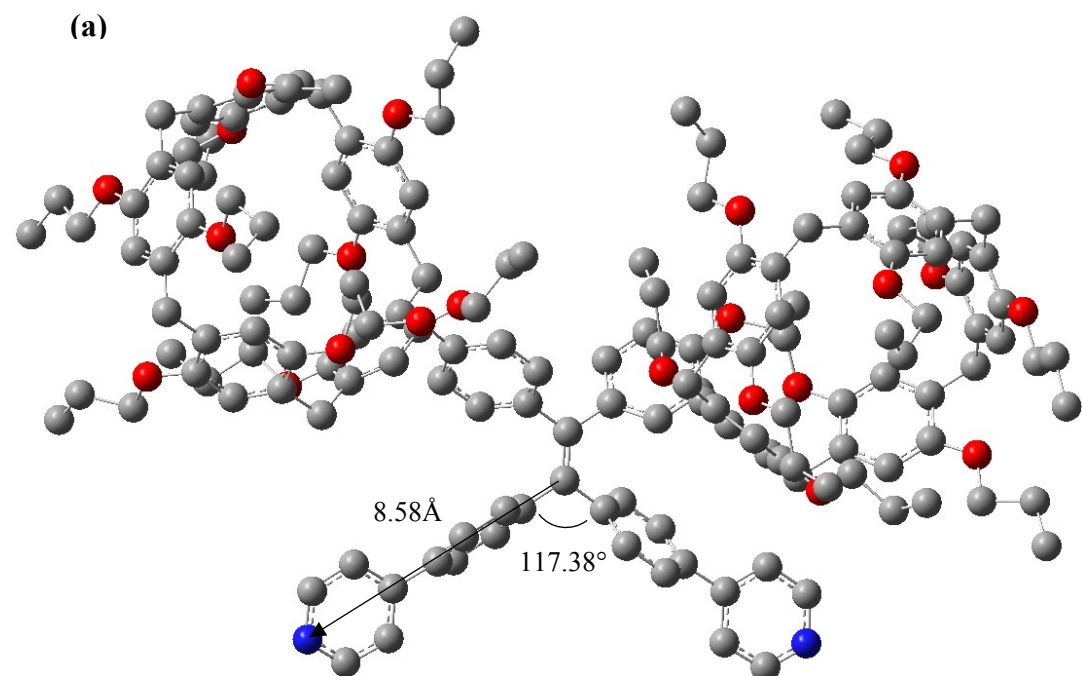


Fig. S1 Ball-and-stick model of the X-ray crystal structure of **2**.

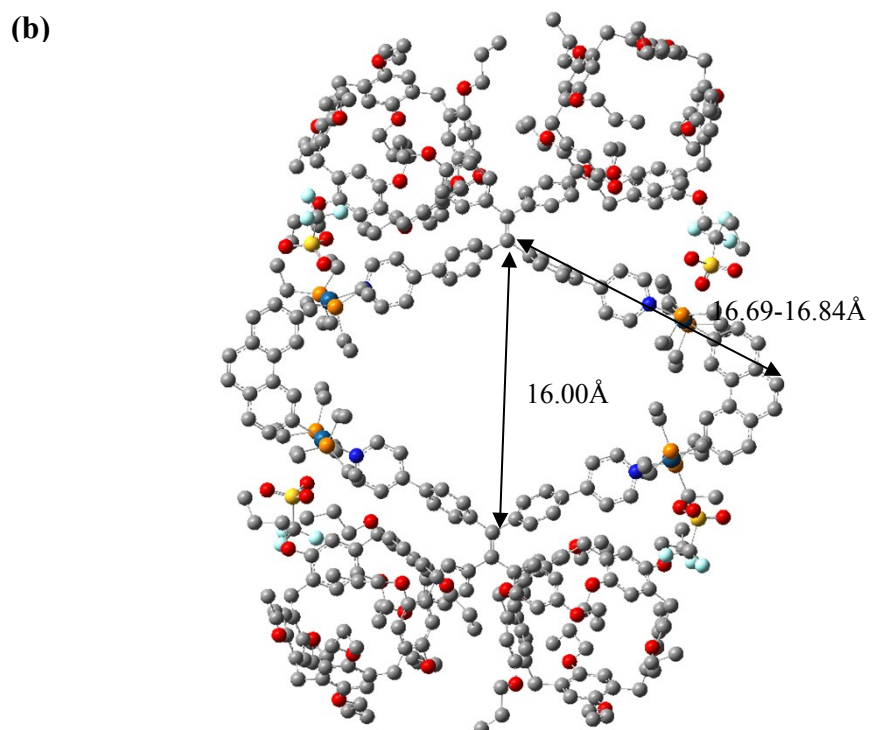
Table S1. Crystal data and structure refinement for **2**

Identification code	ta_a
Empirical formula	C ₃₆ H ₂₆ N ₂ O ₂
Formula weight	518.59
Temperature	173(2) K
Wavelength	1.54178 Å
Crystal system, space group	P2(1)/c
Unit cell dimensions	a = 29.8205(5) Å alpha = 90° b = 8.8627(2) Å beta = 110.0500(10)° c = 25.1375(4) Å gamma = 90°
Volume	6240.9(2) Å ³
Z, Calculated density	8, 1.104 Mg/m ³
Absorption coefficient	0.539 mm ⁻¹
F(000)	2176
Crystal size	0.42 x 0.36 x 0.22 mm ³
Theta range for data collection	4.54 to 68.25°
Limiting indices	-35<=h<=35, -10<=k<=10, -29<=l<=30
Reflections collected / unique	55019 / 11413 [R(int) = 0.0529]
Completeness to theta = 25.01°	99.8 %
Absorption correction	Semi-empirical from equivalents
Max. and min. transmission	0.8906 and 0.8052
Refinement method	Full-matrix least-squares on F ²
Data / restraints / parameters	11413 / 0 / 725
Goodness-of-fit on F ²	1.049
Final R indices [I>2sigma(I)]	R1 = 0.0509, wR2 = 0.1235
R indices (all data)	R1 = 0.0756, wR2 = 0.1329
Largest diff. peak and hole	0.837 and -0.177 e.Å ⁻³

4. The simulated molecular model of H1, H2 and H3.

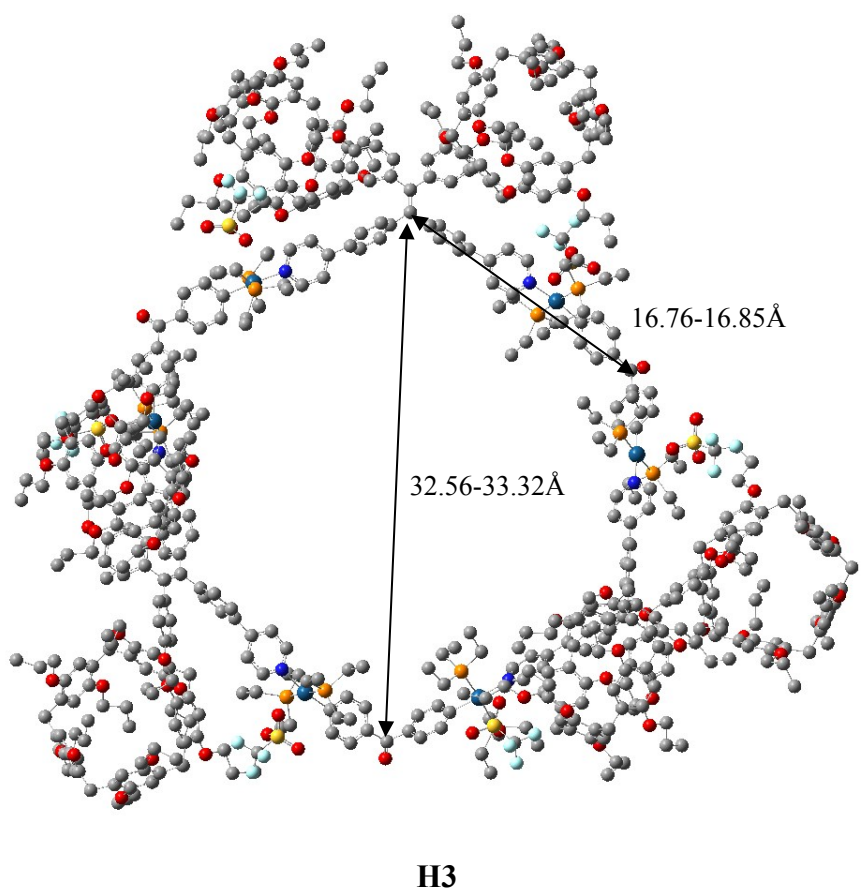


H1



H2

(C)



H3

Fig. S2 The geometry structures of (a) H1, (b) H2 and (c) H3 optimized by PM6 semiempirical molecular orbital method.

5. 2-D ^1H - ^1H NOESY NMR spectra of H2 and H3 in acetone- d_6

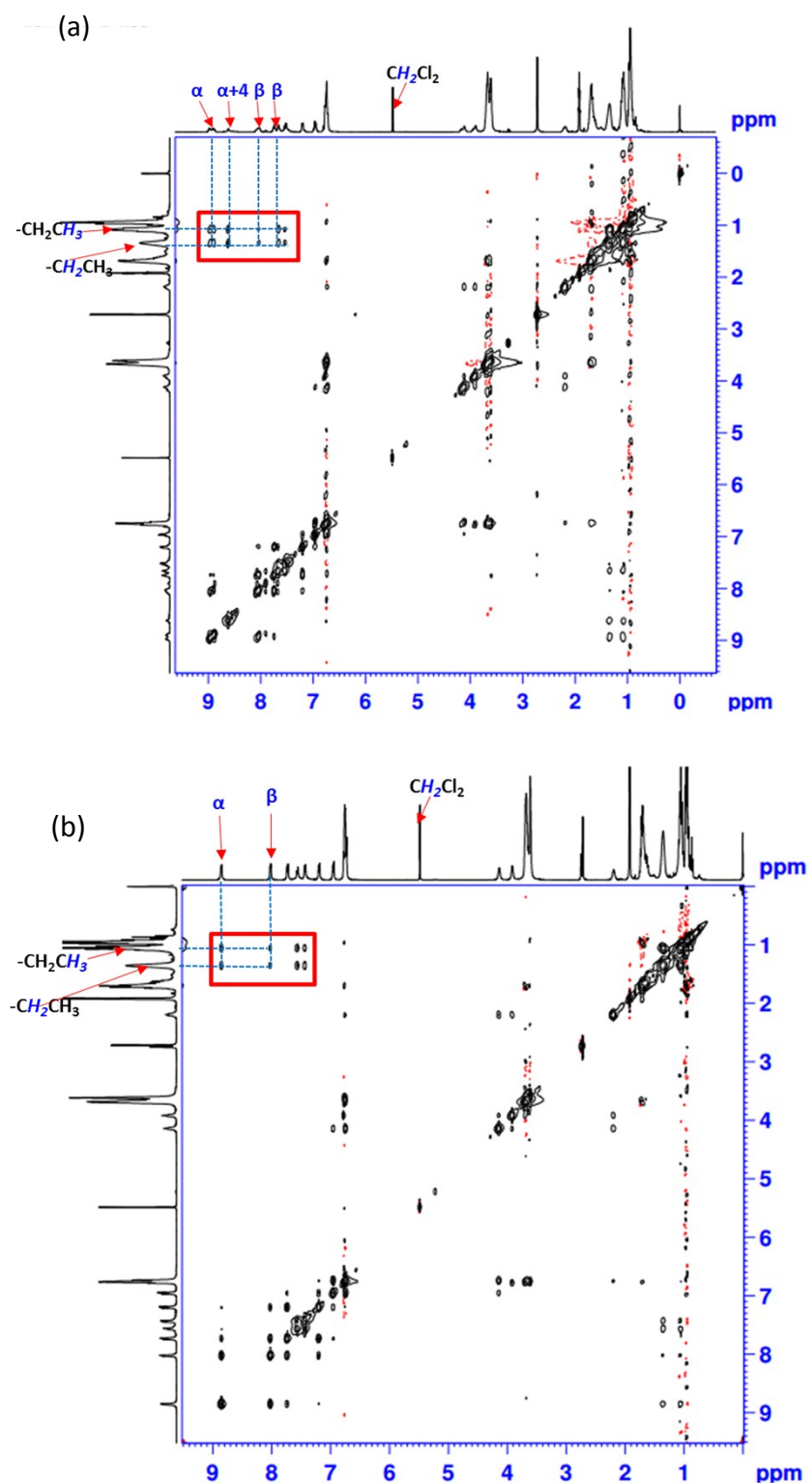


Fig. S3 (a) 2D ^1H - ^1H NOESY NMR spectra of (a) 5.0 mM **H2** and (a) 3.3 mM **H3** in acetone- d_6 (400 MHz, 295 K)

6. Photophysical investigation of H2 and H3.

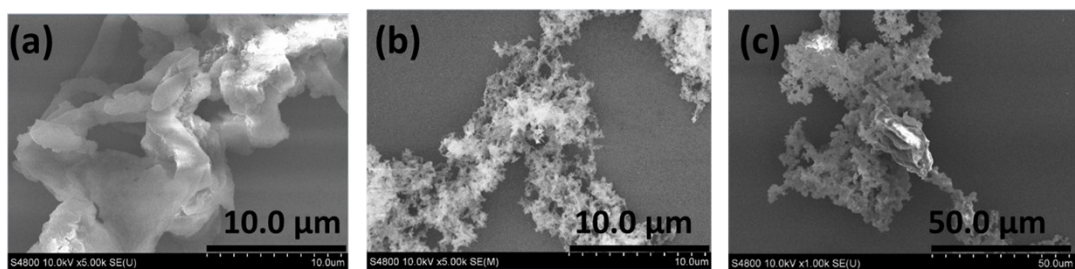


Fig. S4 SEM images of the aggregates of (a) **H1**, (b) **H2** and (c) **H3** formed in the acetone/water mixtures containing 90% water.

7. Host-guest complexation studies in dilute solution.

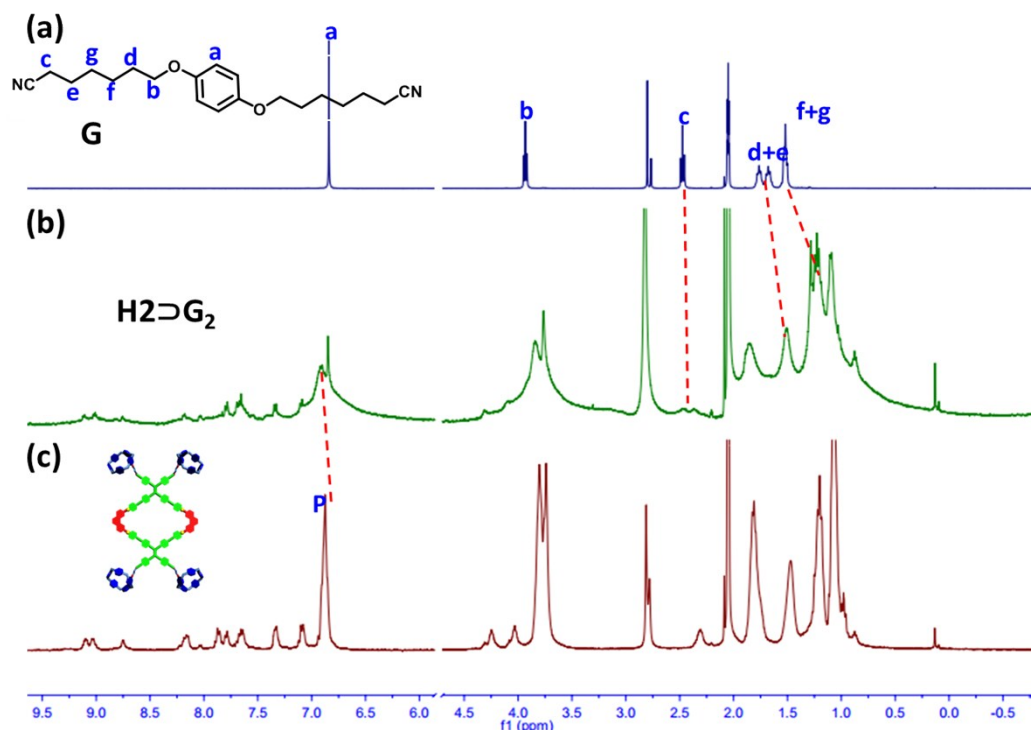


Fig. S5 ¹H NMR spectra (400 MHz, acetone-*d*₆, 295 K) of (a) 3.0 mM **G**, (b) 3.0 mM **G** + 1.5 mM **H2**, (c) 1.5 mM **H2**.

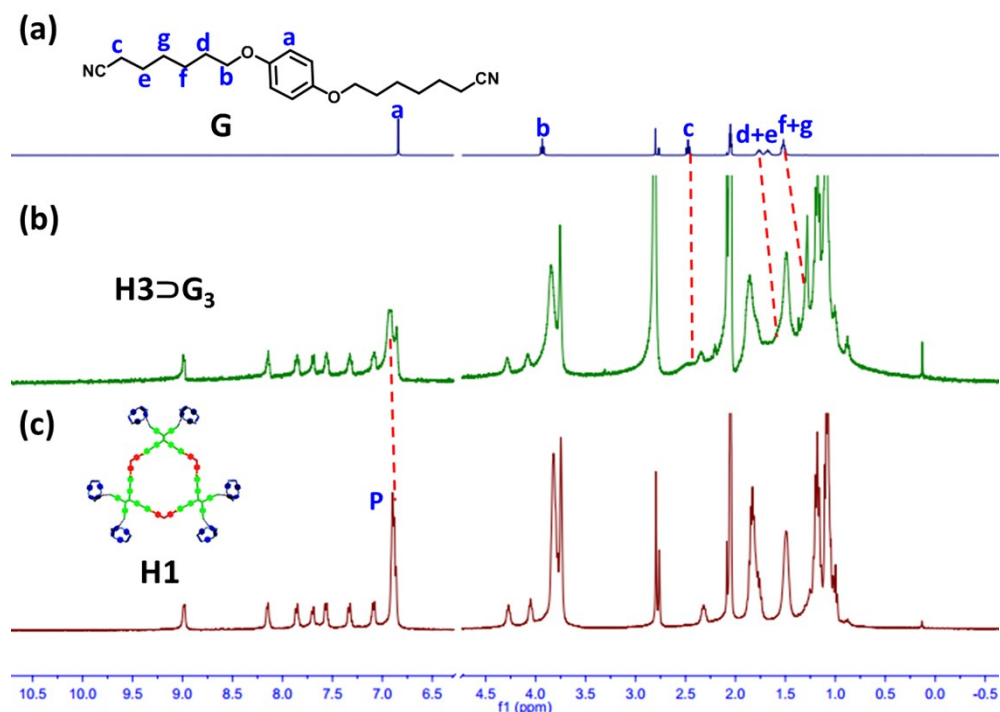


Fig. S6 ^1H NMR spectra (400 MHz, acetone- d_6 , 295 K) of (a) 3.0 mM **G**, (b) 1.6 mM **G** + 1.0 mM **H3**, (c) 1.0 mM **H3**.

7. Cross-linked supramolecular polymers constructed through host-guest interactions

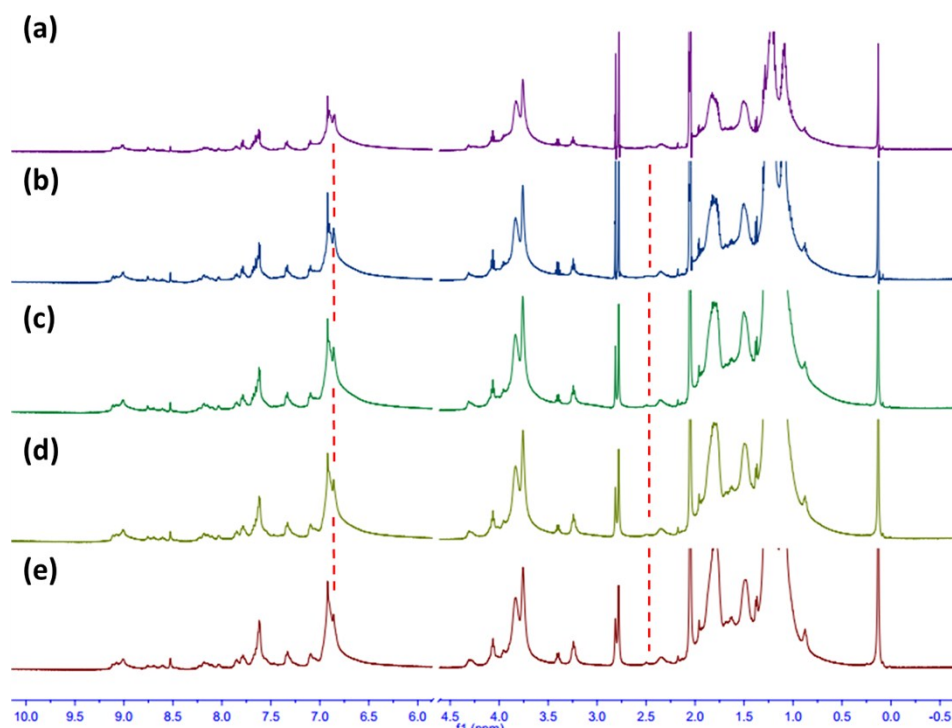


Fig. S7 ^1H NMR spectra of $\text{H}2 \supset \text{G}_2$ (500 MHz, acetone- d_6 , 295 K) at different concentrations: (a) 4.0 mM, (b) 8.0 mM, (c) 12.0 mM, (d) 16.0 mM, (e) 20.0 mM.

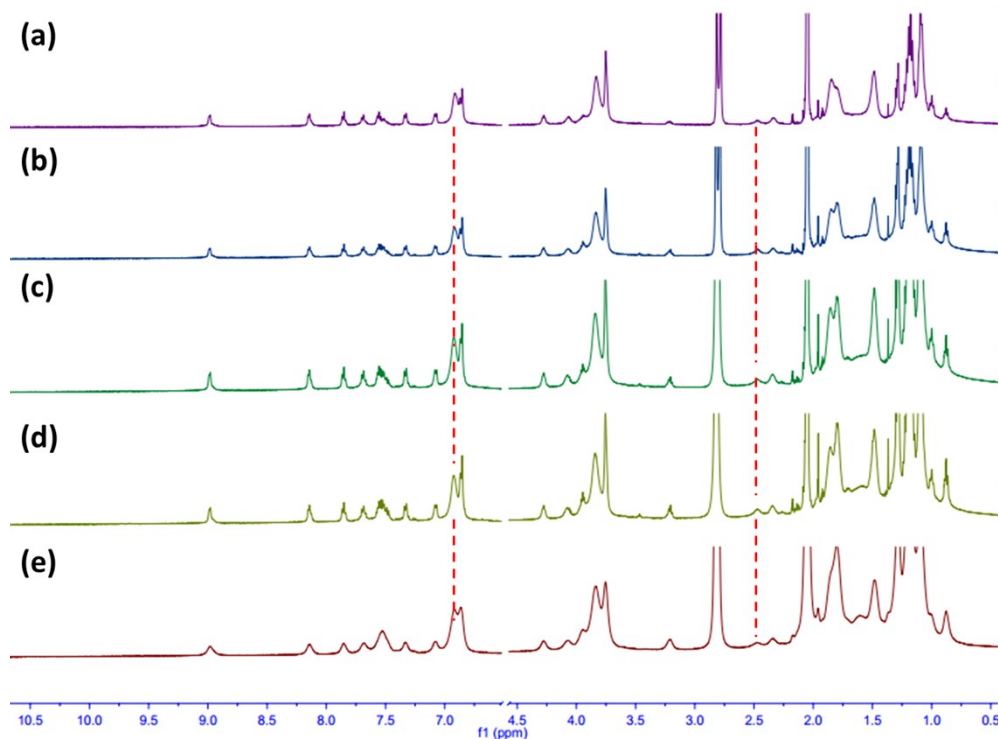


Fig. S8 ^1H NMR spectra of $\text{H3}\rhd\text{G}_3$ (500 MHz, acetone- d_6 , 295 K) at different concentrations: (a) 4.0 mM, (b) 8.0 mM, (c) 12.0 mM, (d) 16.0 mM, (e) 20.0 mM.

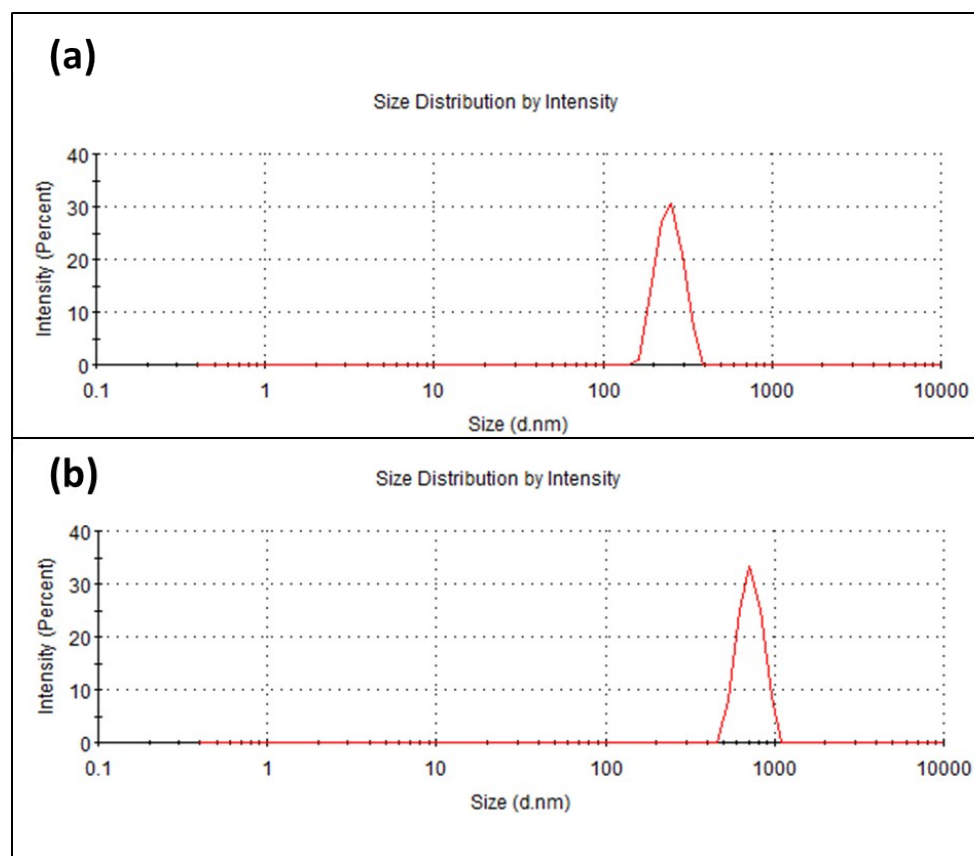


Fig. S9 DLS results: (a) $\text{H2}\rhd\text{G}_2$ (the concentration of pillar[5]arene unit is 4 mM), (b) $\text{H3}\rhd\text{G}_3$ (the concentration of pillar[5]arene unit is 6 mM).

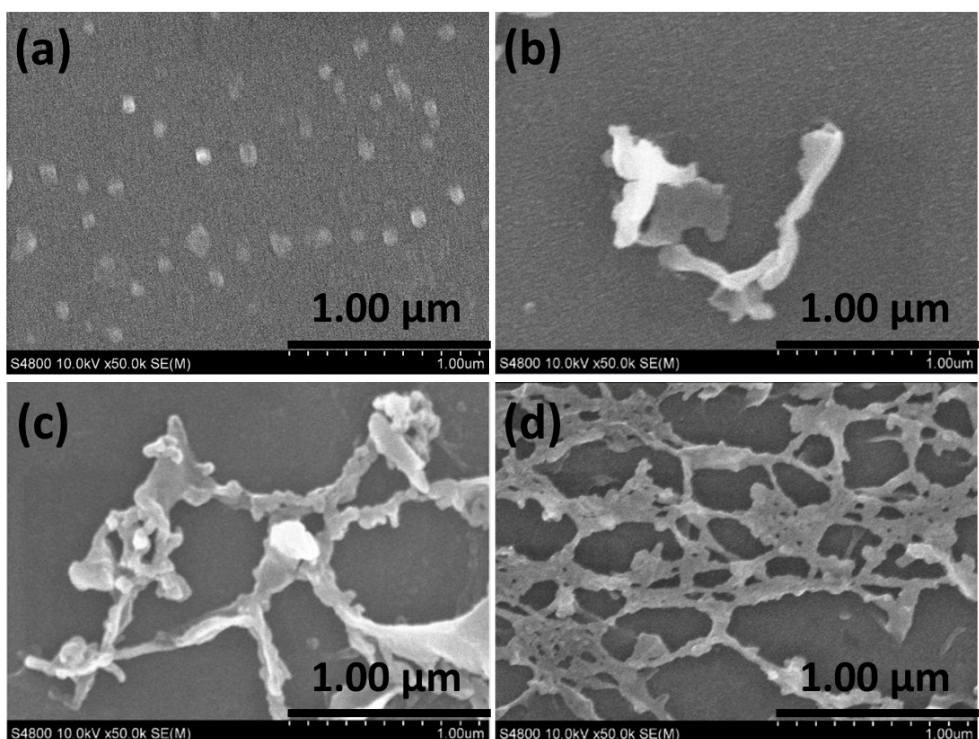


Fig. S10 Concentration-dependent SEM images of supramolecular polymers $\mathbf{H}_2 \supset \mathbf{G}_2$ (a) ca. 0.1 mM; (b) ca. 0.5 mM; (c) ca. 1.0 mM; (d) ca. 5.0 mM.

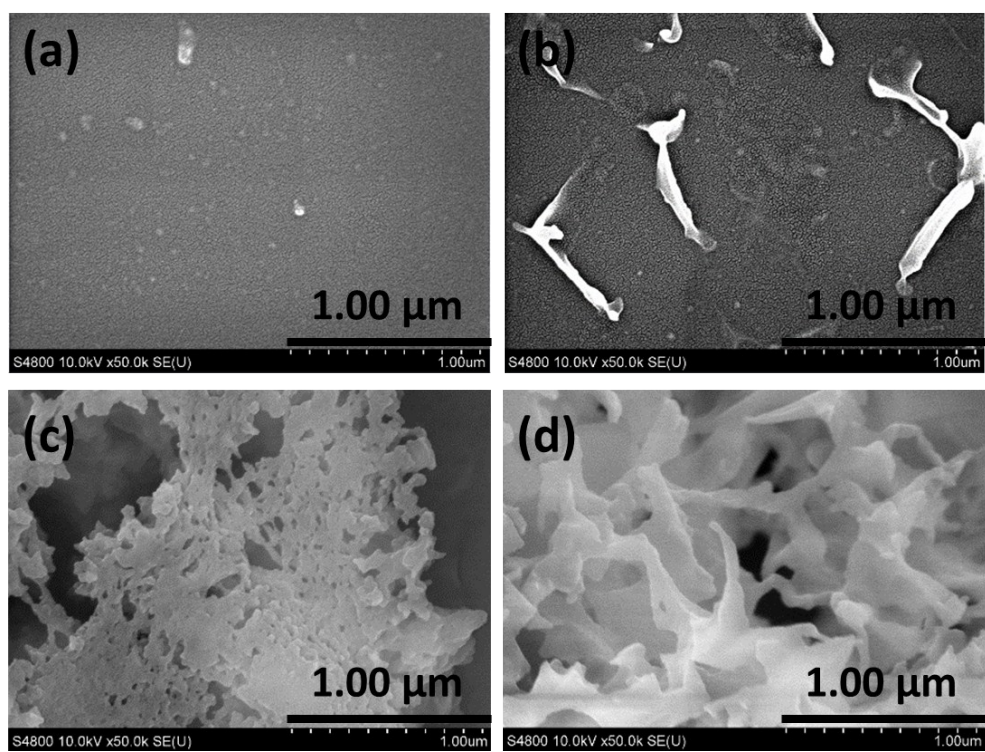


Fig. S11 Concentration-dependent SEM images of supramolecular polymers $\mathbf{H}_3 \supset \mathbf{G}_3$ (a) ca. 0.1 mM; (b) ca. 0.5 mM; (c) ca. 1.0 mM; (d) ca. 5.0 mM.

8. Stimuli-responsive supramolecular polymer gels

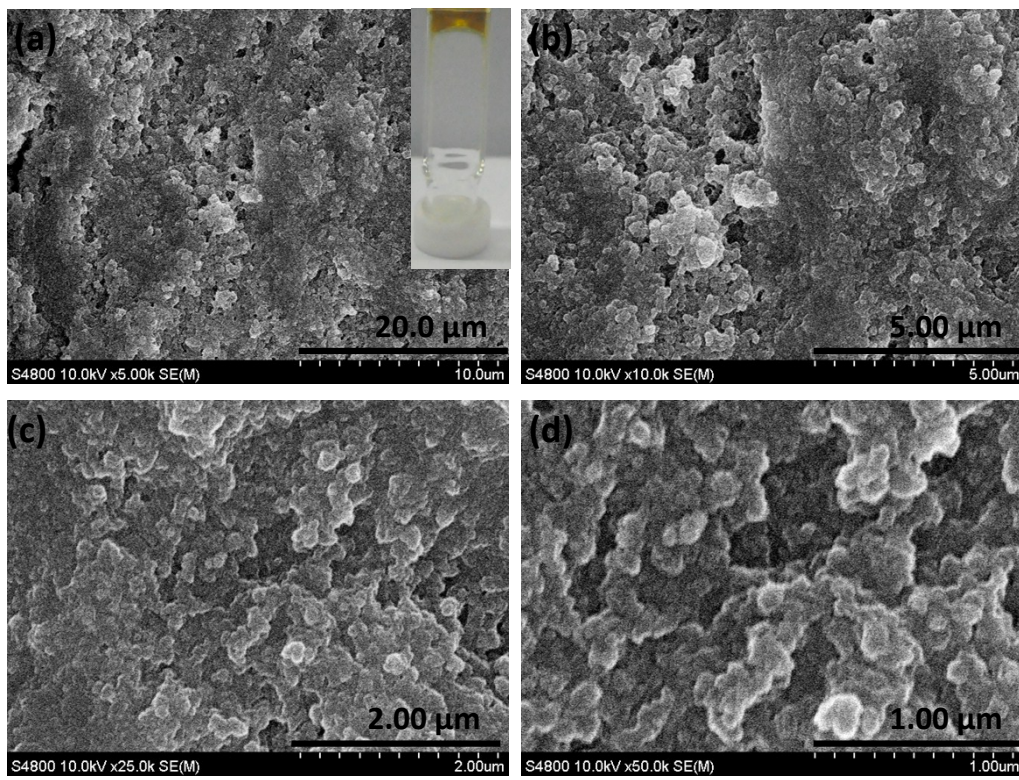


Fig. S12 SEM images of supramolecular gels H₂⊃G₂ which under different scale bars in acetone.

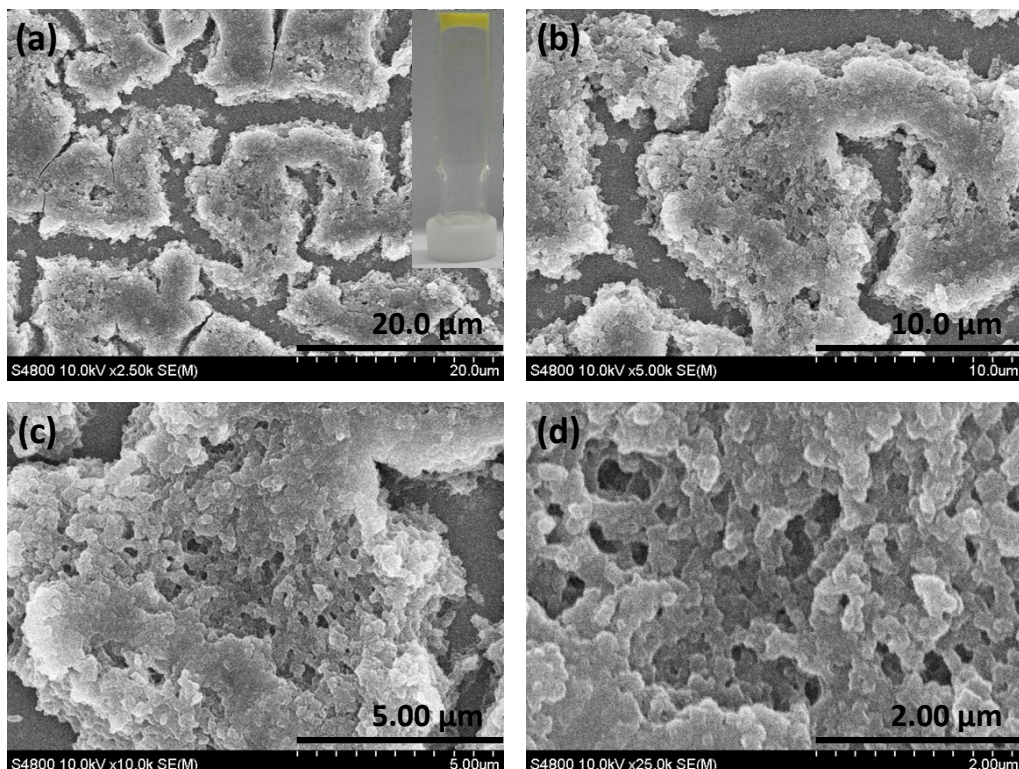


Fig. S13 SEM images of supramolecular gels H₃⊃G₃ which under different scale bars in acetone.

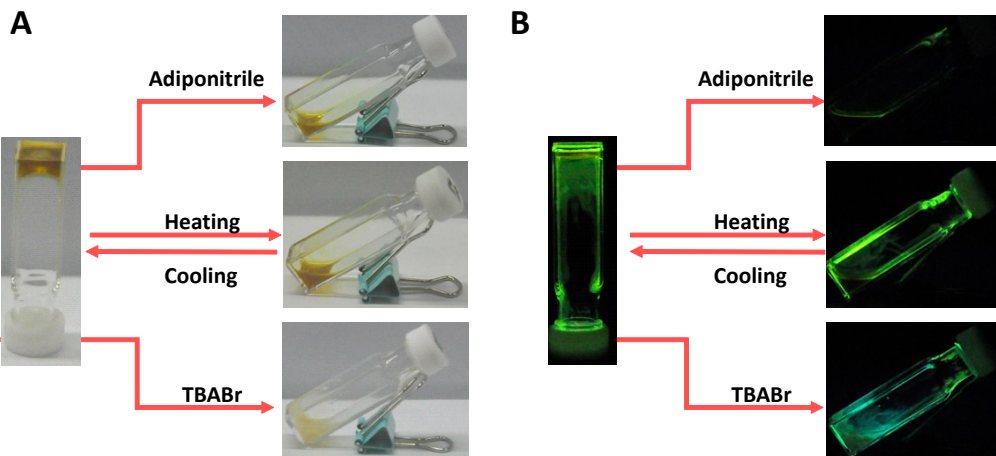


Fig. S14 Gel–sol transitions of supramolecular polymer gel $\mathbf{H2}\supset\mathbf{G}_2$ triggered by a variety of stimuli.

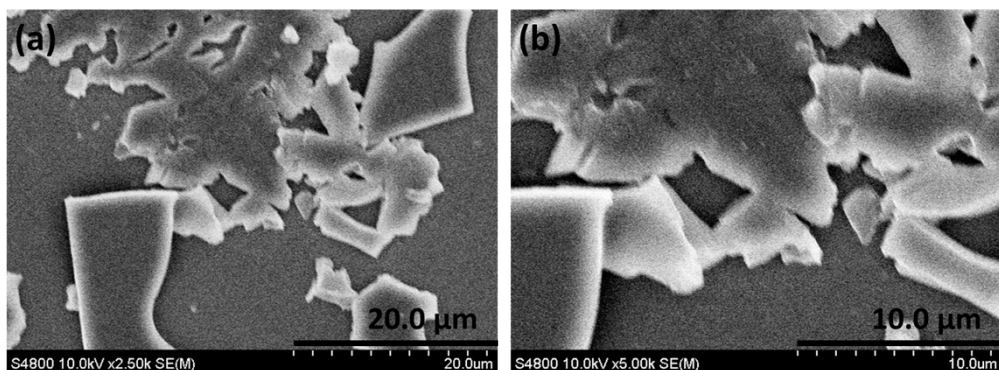


Fig. S15 SEM images of the destroyed supramolecular gels $\mathbf{H2}\supset\mathbf{G}_2$ after the addition of adiponitrile (1.0 eq to the pillar[5]arene unit).

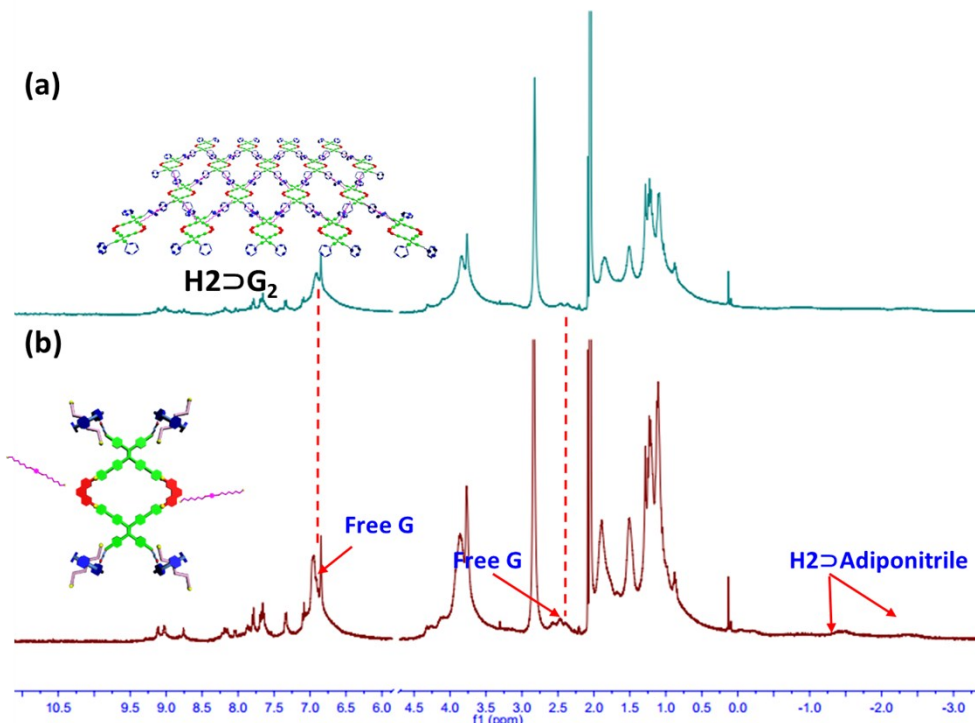


Fig. S16 ^1H NMR spectra showing the disassembly of polymer networks (400 MHz, 295 K, acetone- d_6): (a) supramolecular polymer $\mathbf{H2}\supset\mathbf{G}_2$, (b) after the addition of equimolar adiponitrile to $\mathbf{H2}\supset\mathbf{G}_2$.

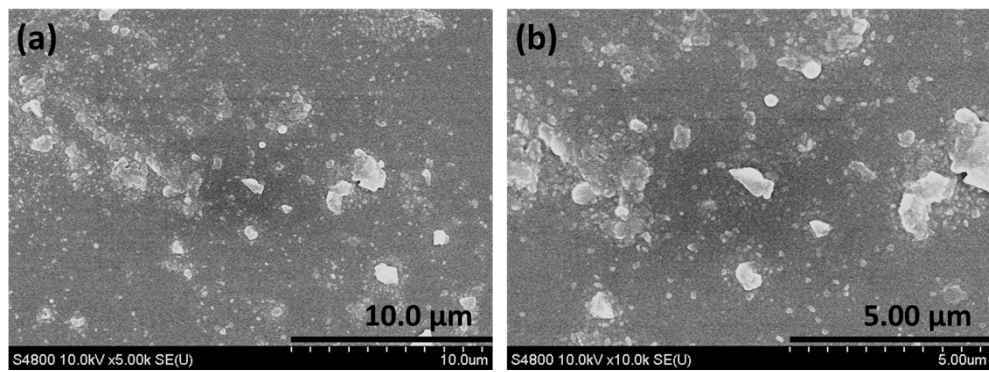


Fig. S17 SEM images of the destroyed supramolecular gels $\mathbf{H}2\supset\mathbf{G}_2$ after the addition of TBABr (1.0 eq to the pillar[5]arene unit).

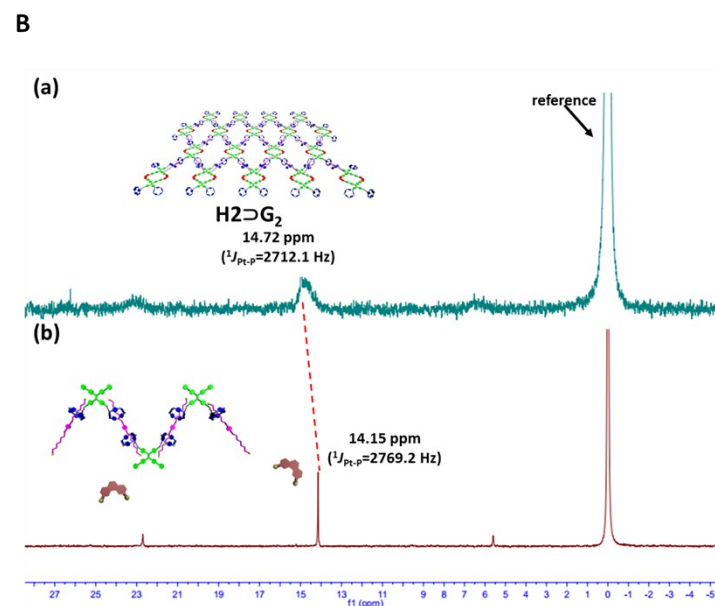
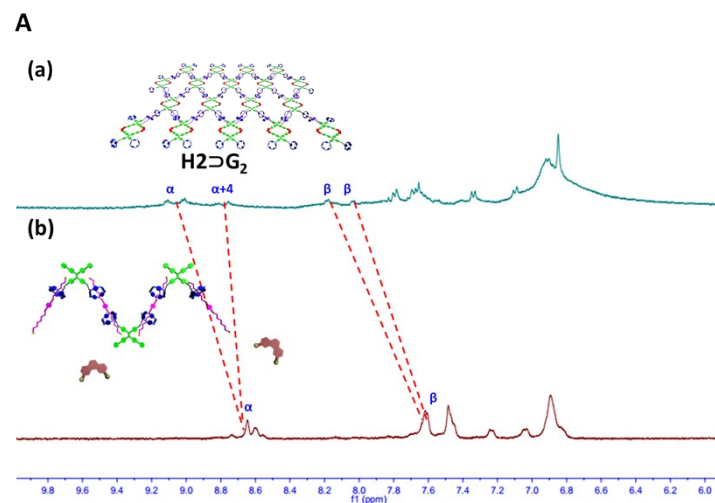


Fig. S18 (A) ^1H and (B) ^{31}P NMR spectra showing the disassembly of supramolecular polymer networks (400 MHz, acetone- d_6 , 295 K): (a) supramolecular polymer $\mathbf{H}2\supset\mathbf{G}_2$, (b) after the addition of two equivalents of TBABr to $\mathbf{H}2\supset\mathbf{G}_2$.

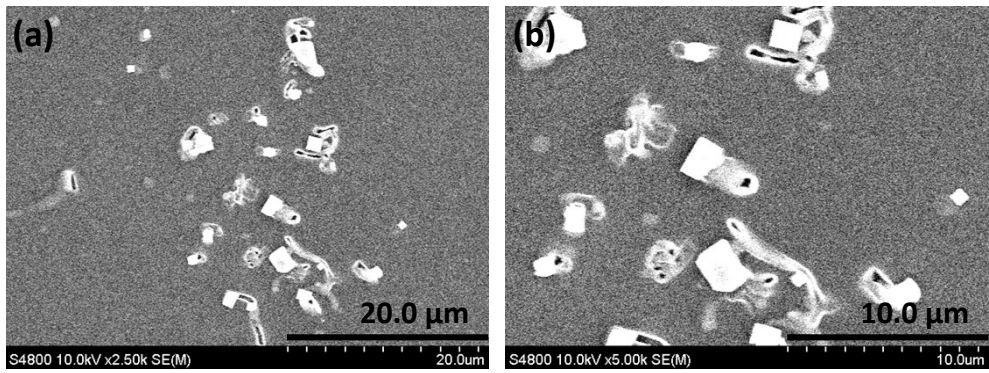


Fig. S19 SEM images of the destroyed supramolecular gels $\mathbf{H3}\supset\mathbf{G}_3$ after the addition of adiponitrile (1.0 eq to the pillar[5]arene unit).

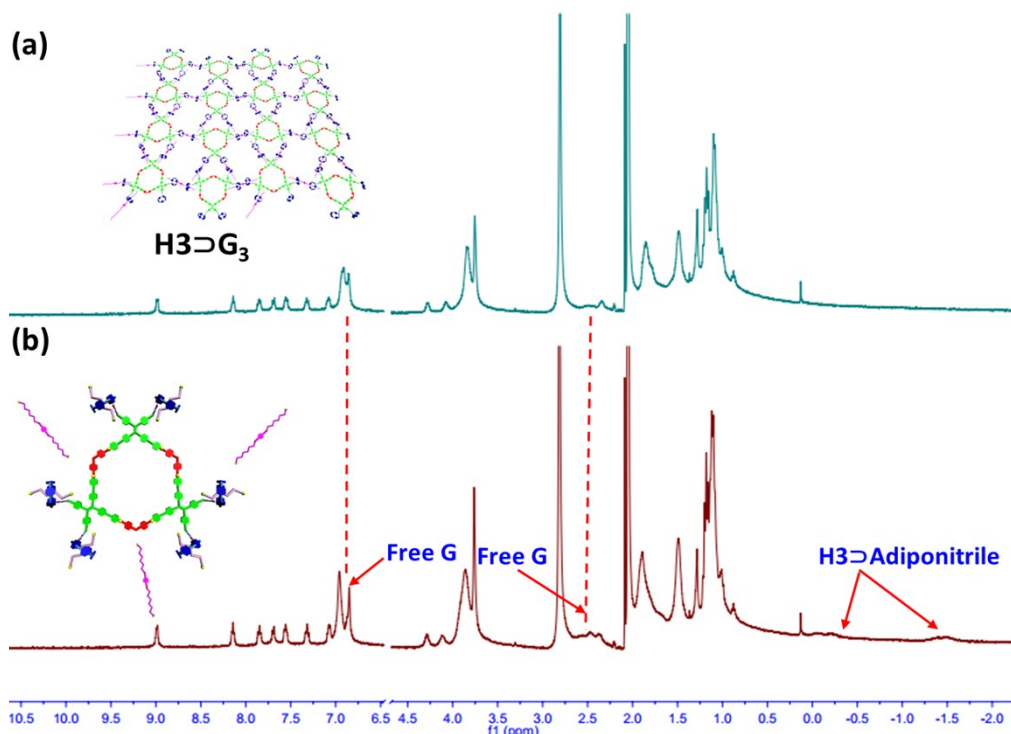


Fig. S20 ^1H NMR spectra showing the disassembly of polymer networks (400 MHz, 295 K, acetone- d_6): (a) supramolecular polymer $\mathbf{H3}\supset\mathbf{G}_3$, (b) after the addition of equimolar adiponitrile to $\mathbf{H3}\supset\mathbf{G}_3$.

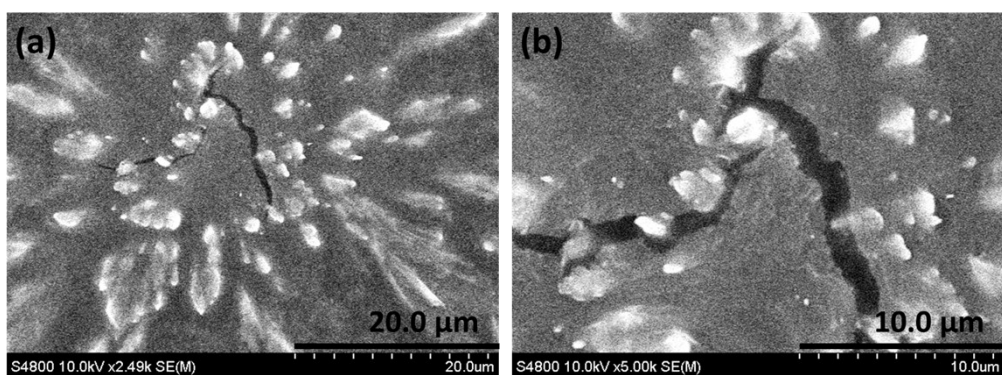


Fig. S21 SEM images of the destroyed supramolecular gels $\mathbf{H3}\supset\mathbf{G}_3$ after the addition of TBABr (1.0 eq to the pillar[5]arene unit).

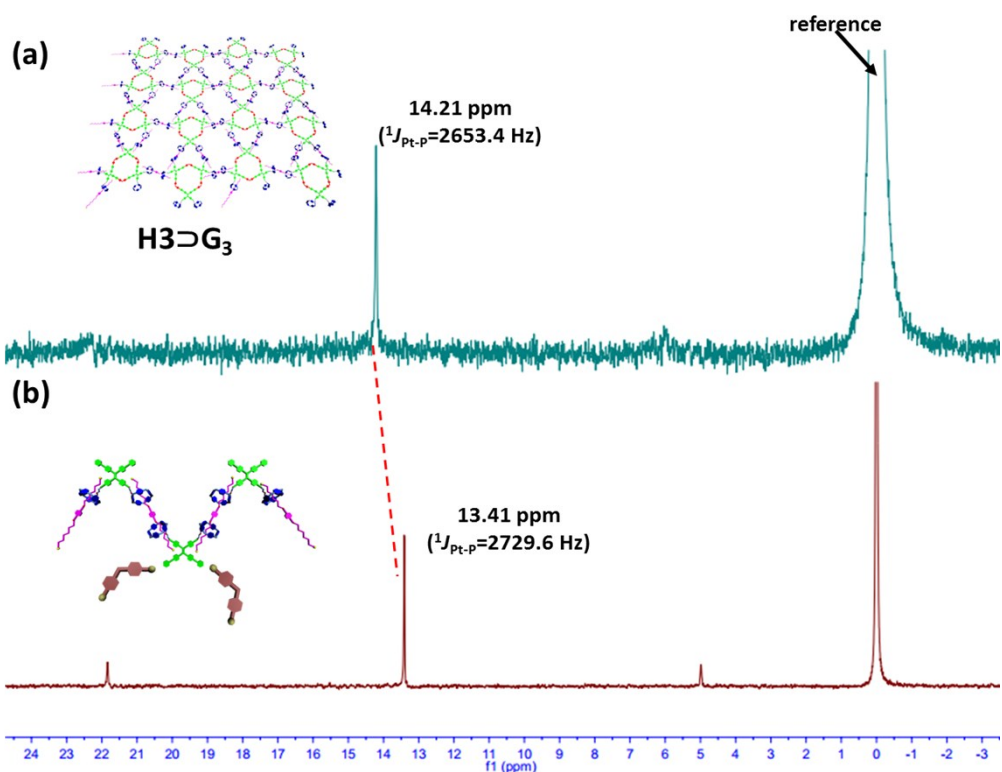
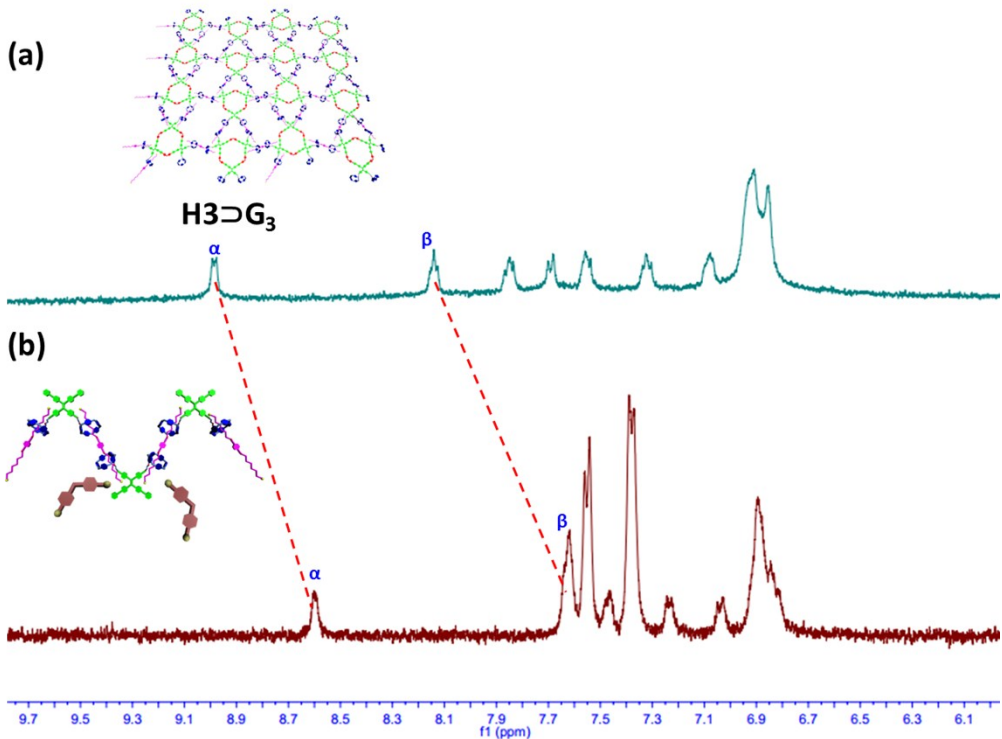


Fig. S22 (A) ^1H and (B) ^{31}P NMR spectra showing the disassembly of supramolecular polymer networks (400 MHz, acetone- d_6 , 295 K): (a) supramolecular polymer **H3 \supset G₃**, (b) after the addition of two equivalents of TBABr to **H3 \supset G₃**.

9. Multiple nuclear NMR (^1H , ^{31}P , ^{19}F , and ^{13}C NMR) spectra of new compounds

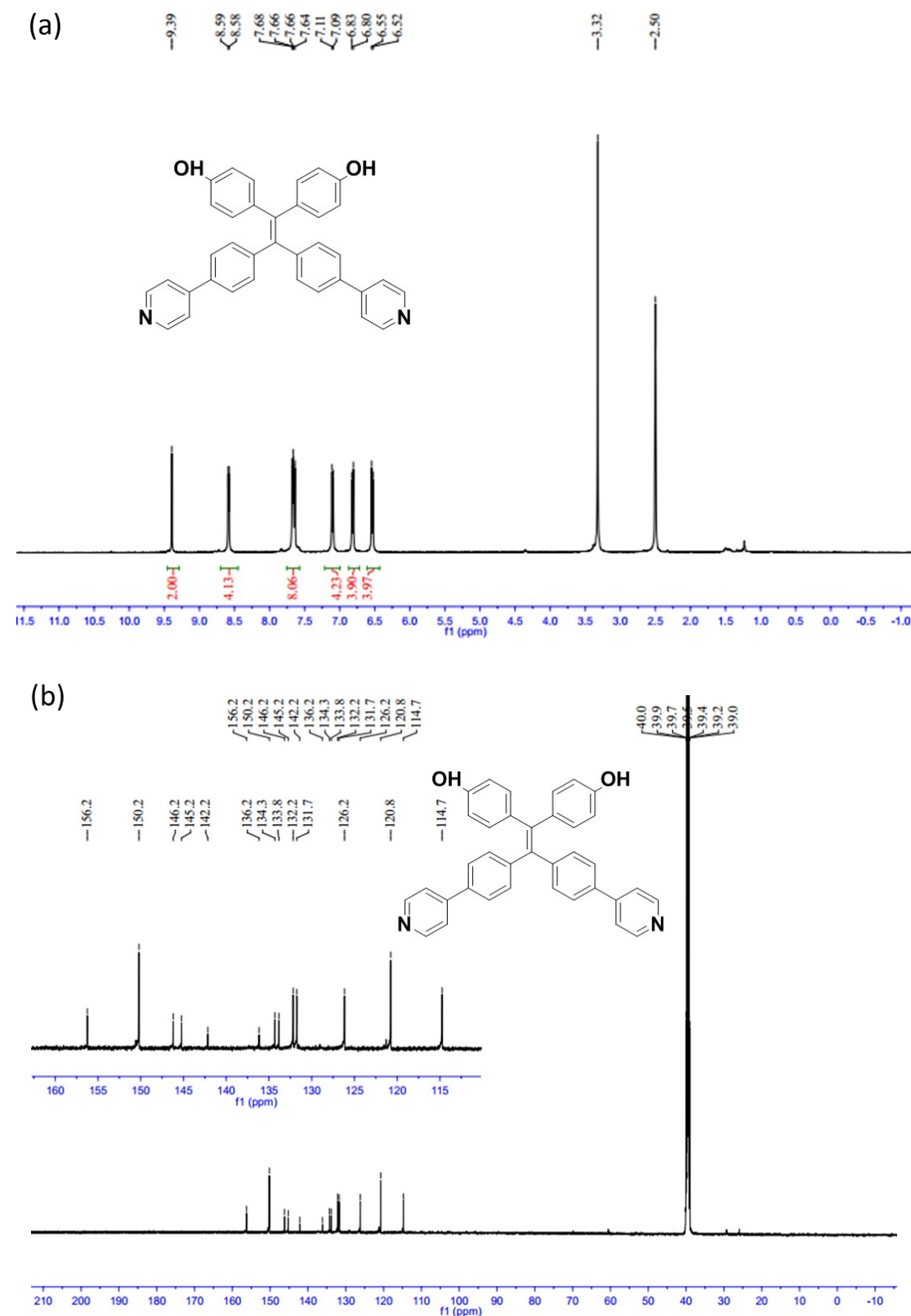
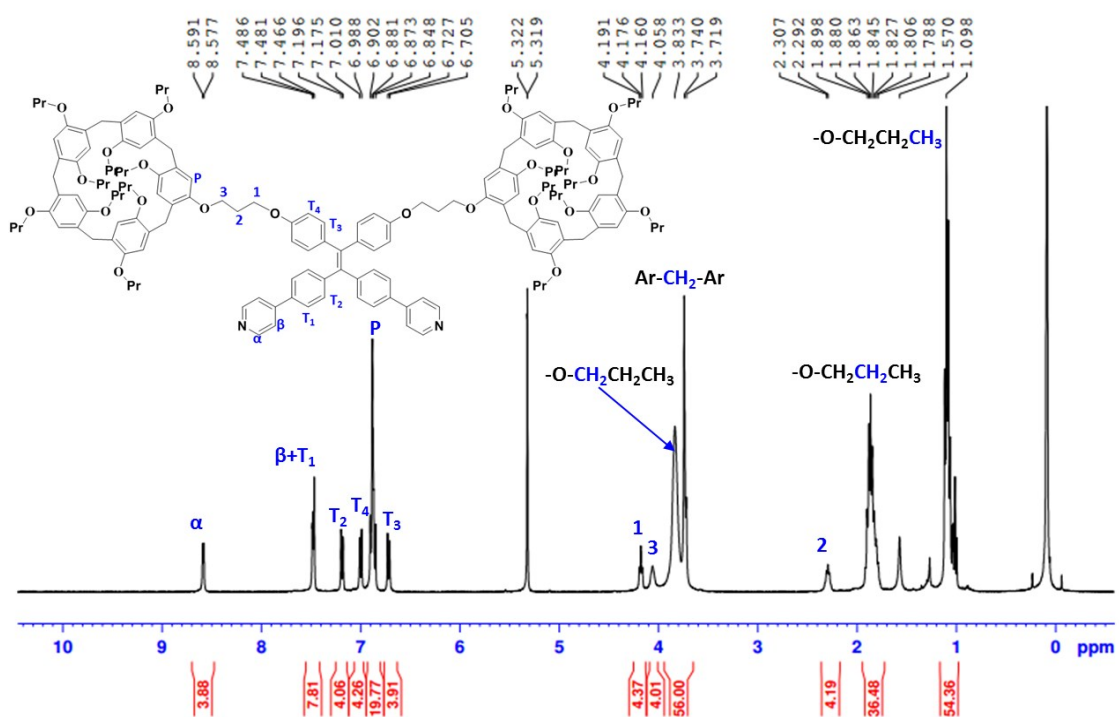


Fig. S23 (a) ^1H and (b) ^{13}C NMR spectra of compound 2 in $\text{DMSO}-d_6$

(a)



(b)

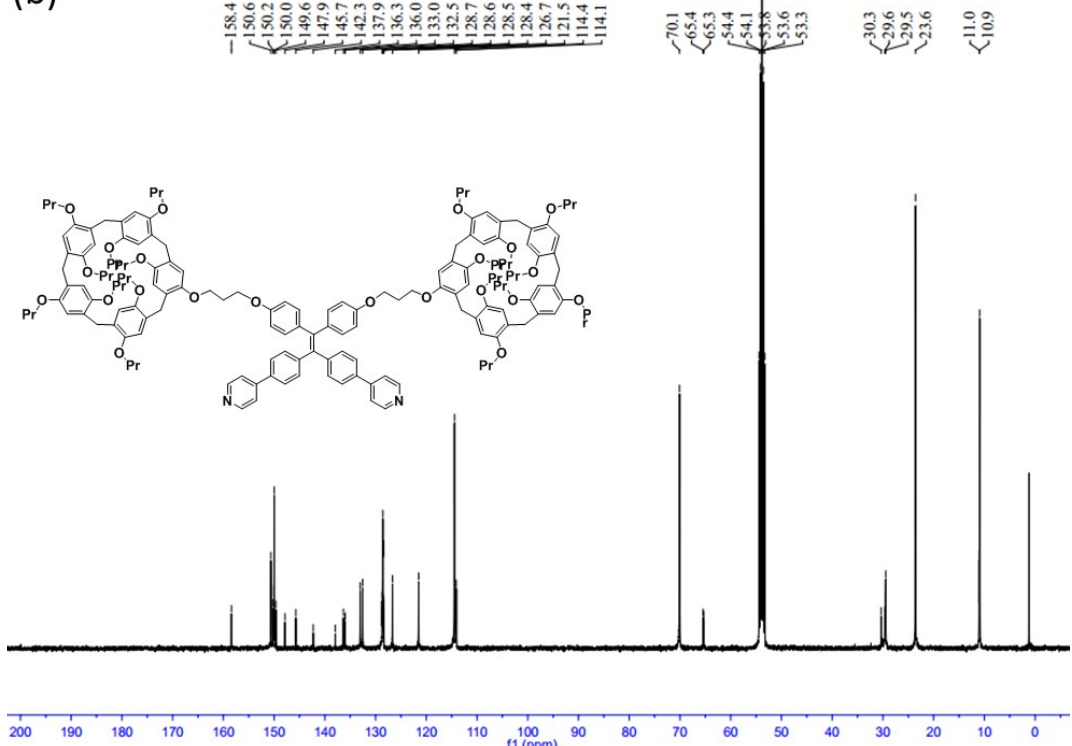
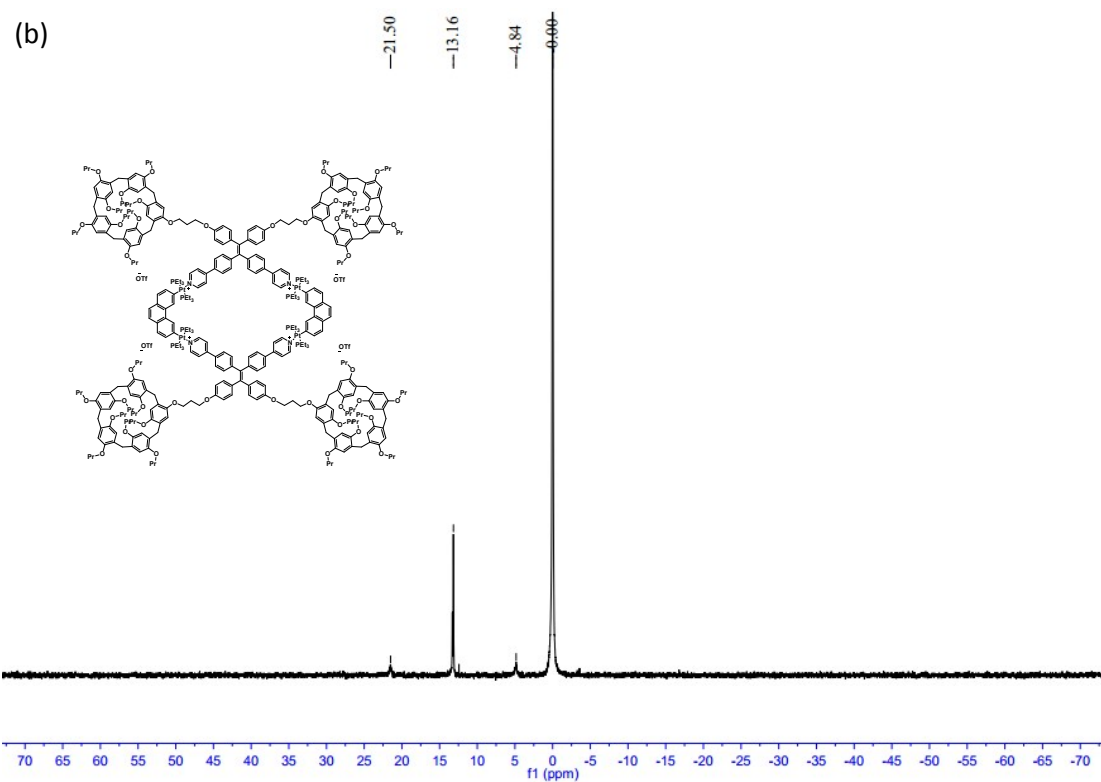
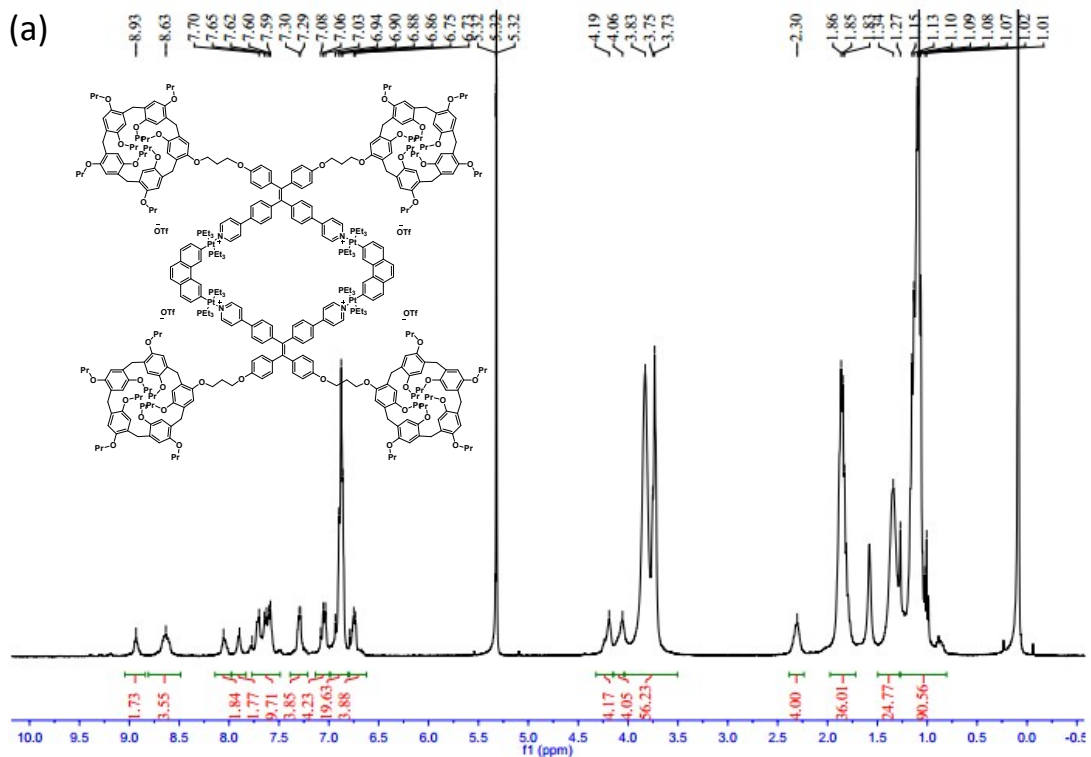


Fig. S24 (a) ¹H (b) ¹³C NMR spectra of H1 in CD_2Cl_2 .



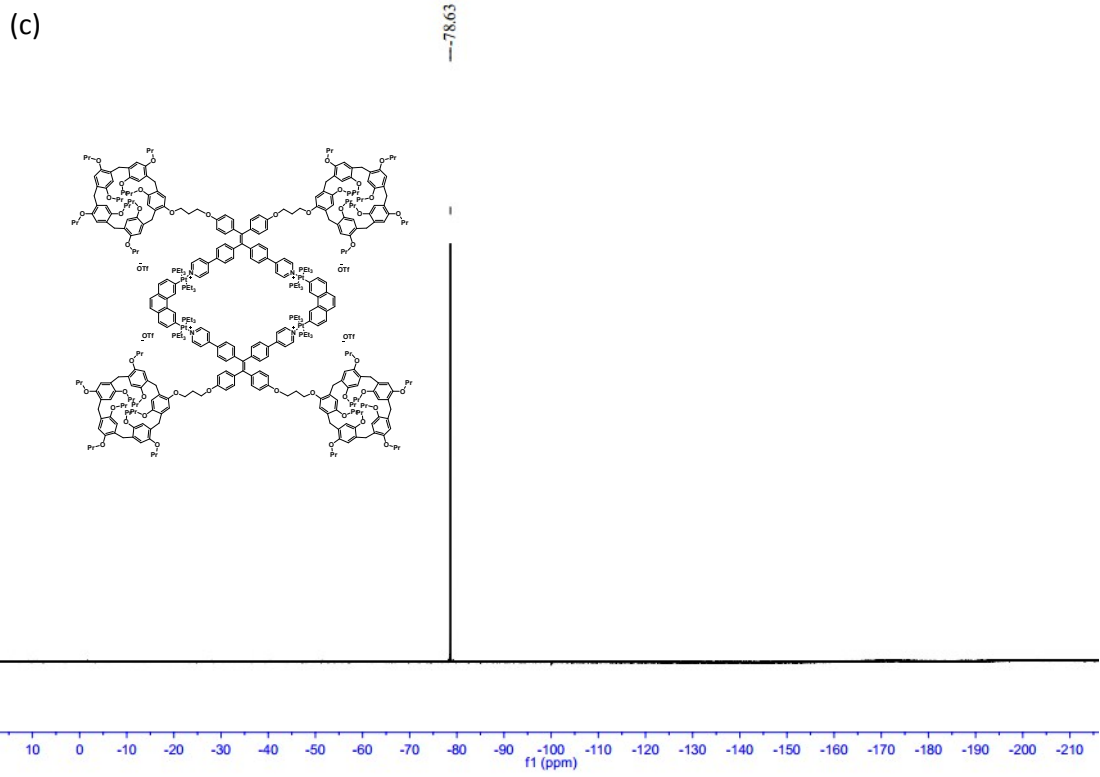
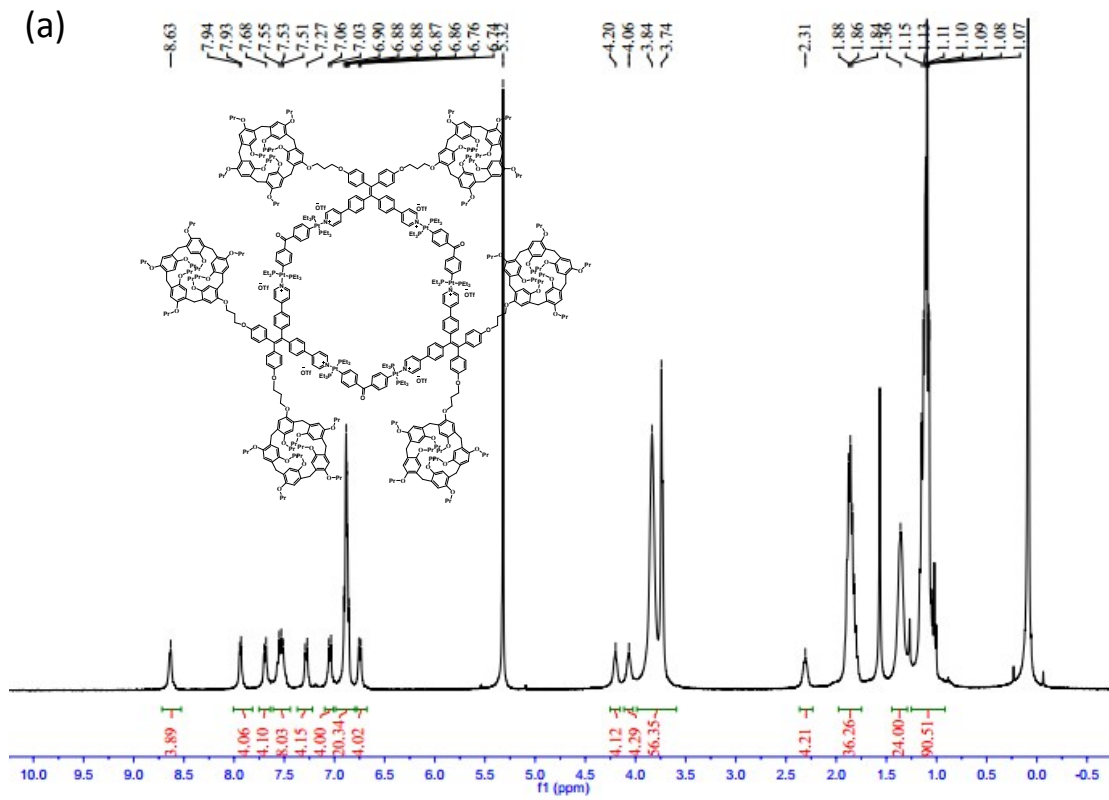


Fig. S25 (a) ¹H, (b) ³¹P and (c) ¹⁹F NMR spectra of H2 in CD₂Cl₂



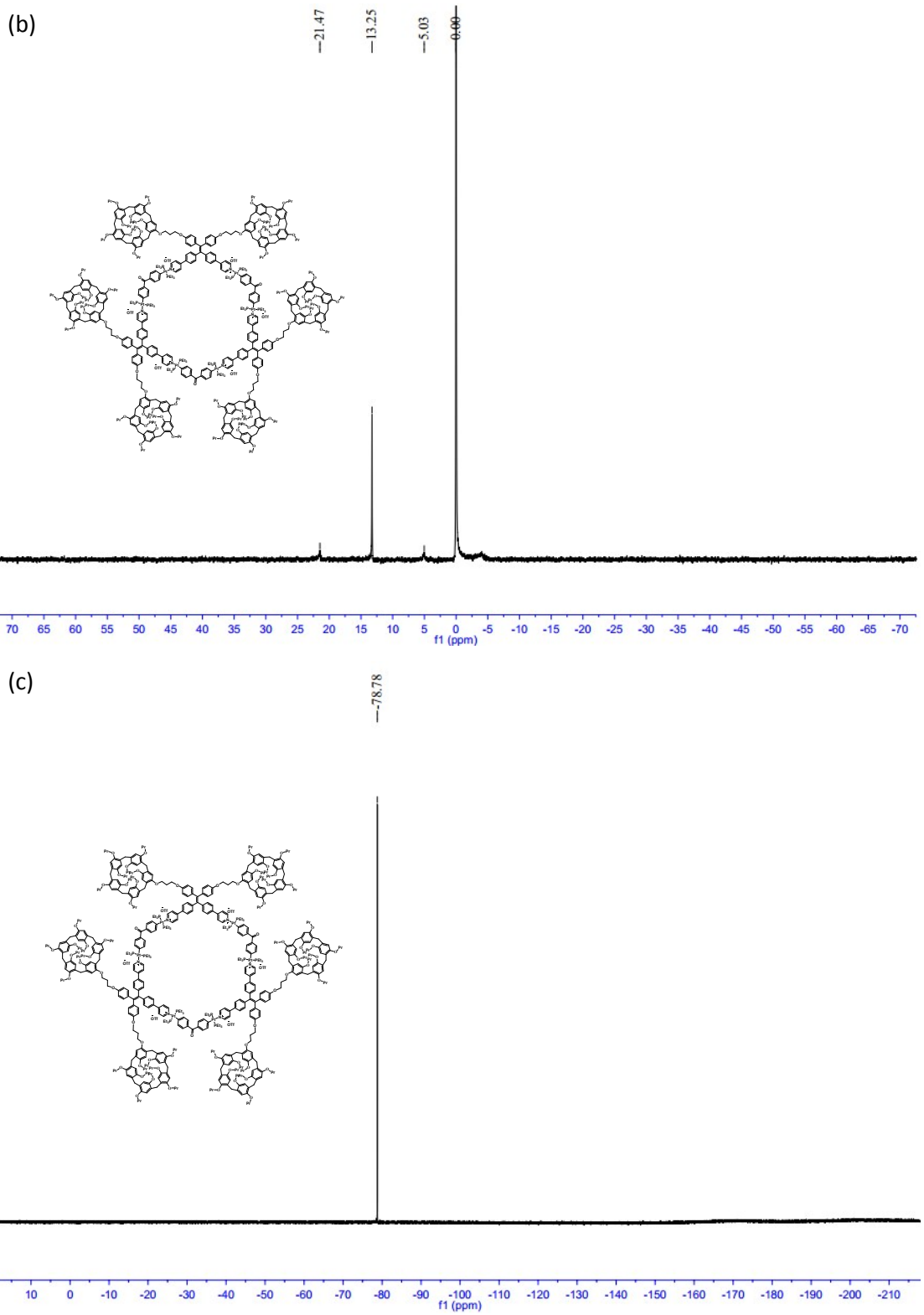


Fig. S26 (a) ^1H , (b) ^{31}P and (c) ^{19}F NMR spectra of **H3** in CD_2Cl_2

11. MS Spectra of New Compounds.

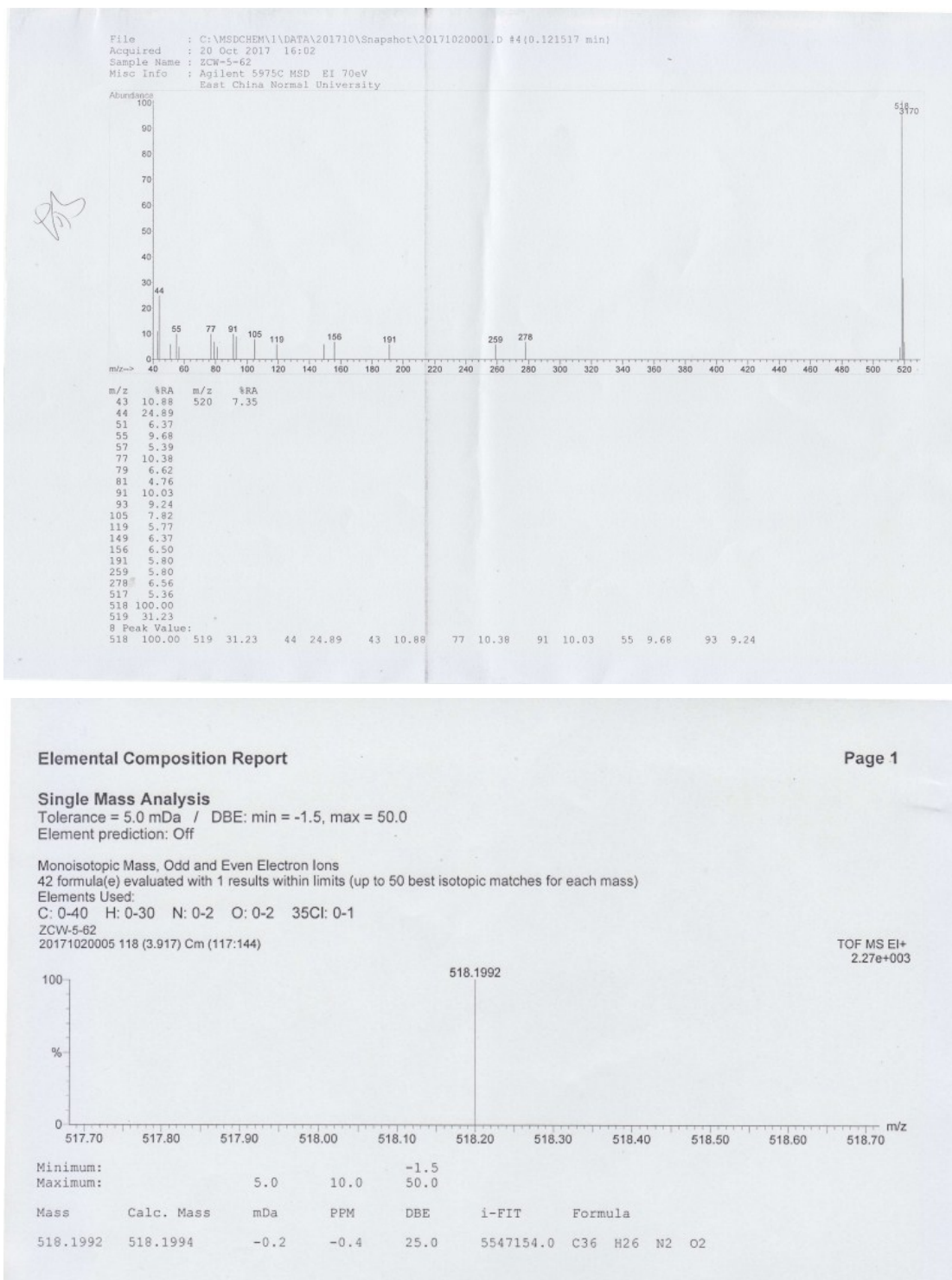


Fig. S27 MS (EI) of **2**: 518 (M^+ , 100), 519 (31), 44 (25), 43 (11), 77 (10), 91 (10), 55 (10), 93 (9); HRMS (EI) of **2**: Exact mass calcd for $C_{36}H_{26}N_2O_2 [M]^+$: 518.1994, Found: 518.1992.

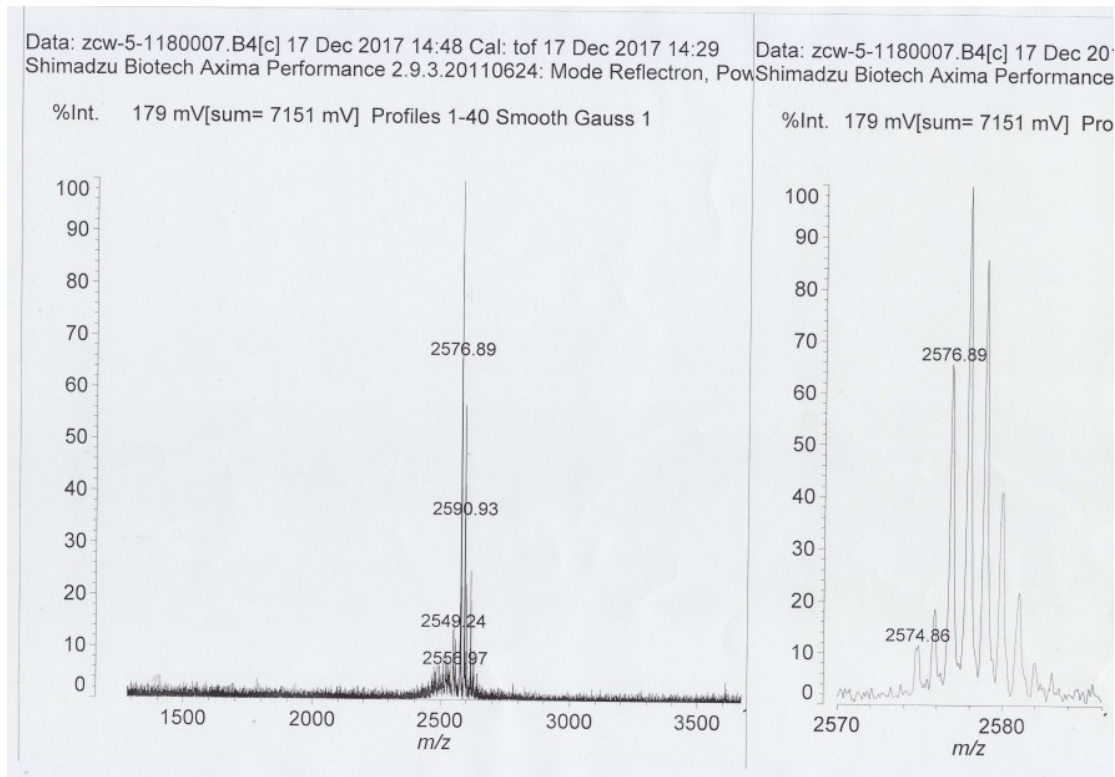


Fig. S28 MOLDI-TOF-MS of compound **H1**: m/z calcd for $C_{166}H_{202}N_2O_{22}$ ($[M+H]^+$): 2576.47, found: 2576.89.

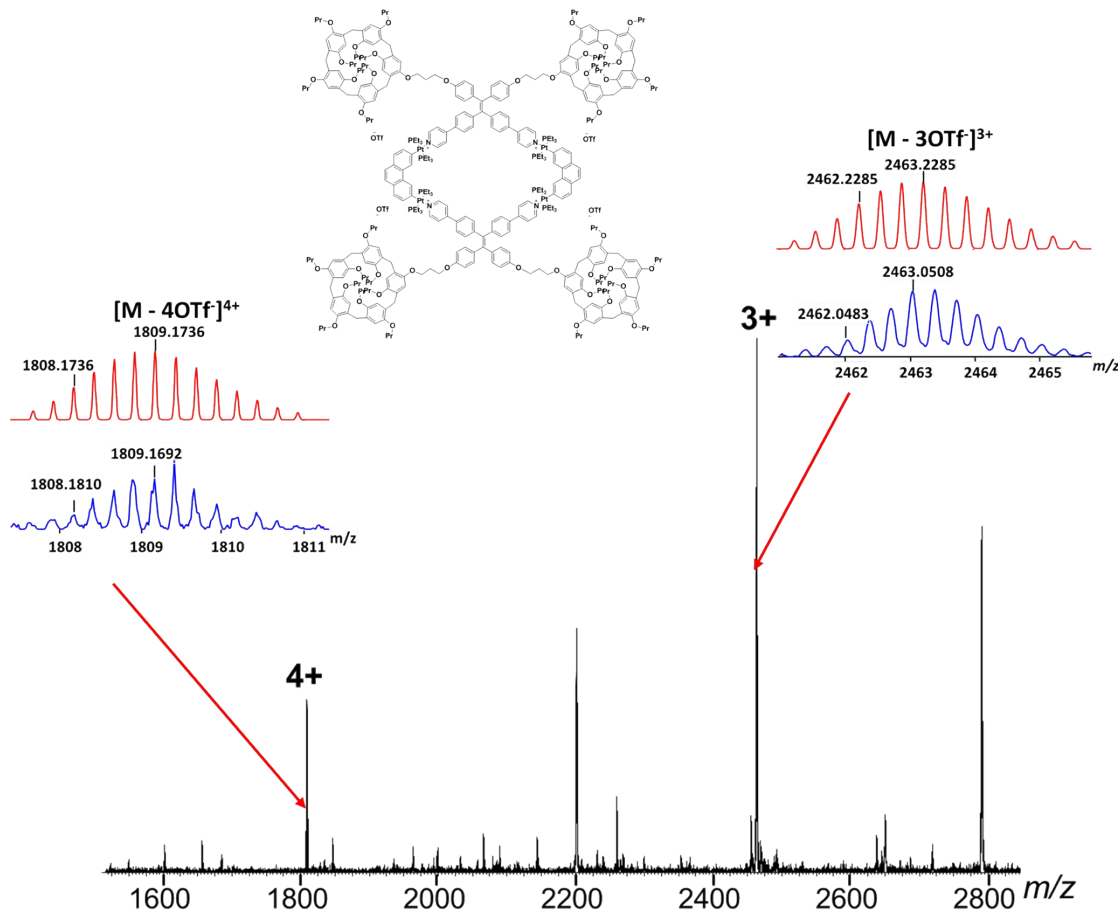


Fig. S29 Experimental ESI-TOF-MS spectra of **H2**(Theoretical (red) and experimental (blue)).

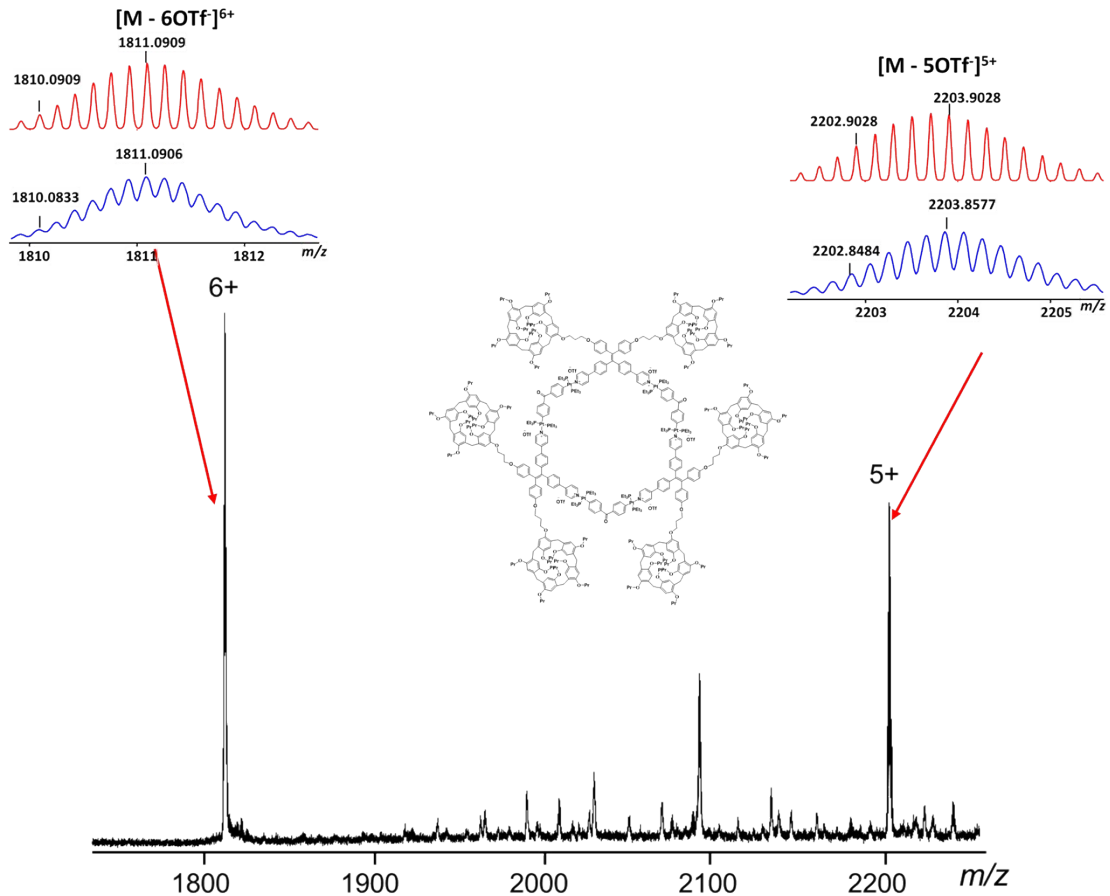


Fig. S30 Experimental ESI-TOF-MS spectra of H3(Theoretical (red) and experimental (blue)).